Liquid-Propellant Rocket Combustion Instability: A Physics-based Multi-fidelity Approach

University of California, Irvine **Pavel Popov, Tuan Nguyen, Juntao Xiong, Jeremy Krieg, Hugh Morgan, Feng Liu, Athanasios Sideris, William A. Sirignano**

Sponsorship by AFOSR **Dr. Mitat Birkan**

LPRE combustion instability involves large-amplitude oscillations in the rocket combustion chamber with potentially disastrous consequences. It is a long-standing problem because every confined gas volume resonates acoustically.

-- Address nonlinear triggering, transient oscillations, and limit-cycle oscillations

-- Uncertainties are magnitude, duration, orientation and location of triggering disturbances.

-- Stochastic processes creating triggers can be fluctuations in propellant flow rates, accelerations, and rogue vortices.

-- Combustion and flow in a liquid-propellant rocket engine (LPRE) forms a complex system.

-- Complex systems involve stochastic behaviors of semi-autonomous components networked allowing emergent behavior to develop.

-- Networked system components are combustor, nozzle, propellant injectors, and all flow and thermal structures.

- ***Emergent structures are large-amplitude acoustic oscillation.***

Content of Presentation

- **Reduced-Dimension Partial Differential Equation**
  - **-- Solution with 10 Co-axial Injectors by CFD**
  - **-- Solution with 10 to 19 Injectors by Nonlinear Perturbation Method**
  - **-- Stochastic Analysis for Triggering Probability**
- **CFD Analysis of Single-Injector Engine**
  - **-- Axisymmetric Analysis of Vortex Dynamics Coupled with Acoustics**
  - **-- Use of Hybrid LES-RANS**
  - **-- Use of Flamelet Theory**
  - **-- Extension of Design to Study Triggering**
- **3D CFD Analysis of 10- to 30-Injector Chamber**
  - **-- Analysis of Vortex Dynamics Coupled with Acoustics**
  - **-- Use of Hybrid LES-RANS**
  - **-- Full-length Nozzle and Injector-port Coupling**
  - **-- Planned Use of Flamelet Theory**
  - **-- Study Triggering**
  - **-- Planned Real-gas study**

Reduced Dimension -- 2D Analysis: Inviscid on large scale, turbulent mixing on injector scale, average over stream direction

Nonlinear Transverse Pressure Wave Equation

$$\frac{\partial^2 p}{\partial t^2} + Ap^{\frac{\gamma-1}{2\gamma}}\frac{\partial p}{\partial t} - Bp^{\frac{\gamma-1}{\gamma}}\left[\frac{\partial^2 p}{\partial r^2} + \frac{1}{r}\frac{\partial p}{\partial r} + \frac{1}{r^2}\frac{\partial^2 p}{\partial \theta^2}\right] = \frac{(\gamma-1)}{\gamma}\frac{1}{p}\left(\frac{\partial p}{\partial t}\right)^2 + (\gamma-1)\frac{\partial E}{\partial t}$$

E is the energy per unit volume per unit time released by combustion and must be modelled. Limit cycles are deterministic but triggers are stochastic.

$$+\gamma p^{\frac{\gamma-1}{\gamma}}\left[\frac{\partial^2 (p^{\frac{1}{\gamma}}u_r^2)}{\partial r^2} + \frac{2}{r}\frac{\partial (p^{\frac{1}{\gamma}}u_r^2)}{\partial r}\right.$$
$$+\frac{2}{r}\frac{\partial^2 (p^{\frac{1}{\gamma}}u_r u_\theta)}{\partial r \partial \theta} + +\frac{2}{r^2}\frac{\partial (p^{\frac{1}{\gamma}}u_r u_\theta)}{\partial \theta}$$
$$\left.+\frac{1}{r^2}\frac{\partial^2 (p^{\frac{1}{\gamma}}u_\theta^2)}{\partial \theta^2} - \frac{1}{r}\frac{\partial (p^{\frac{1}{\gamma}}u_\theta^2)}{\partial r}\right]$$

Momentum equations for radial and azimuthal velocities

$$\frac{\partial u_r}{\partial t} + u_r\frac{\partial u_r}{\partial r} + u_\theta\frac{1}{r}\frac{\partial u_r}{\partial \theta} - \frac{u_\theta^2}{r} + \frac{C}{p^{\frac{1}{\gamma}}}\frac{\partial p}{\partial r} = 0 \qquad \frac{\partial u_\theta}{\partial t} + u_r\frac{\partial u_\theta}{\partial r} + u_\theta\frac{1}{r}\frac{\partial u_\theta}{\partial \theta} + \frac{u_r u_\theta}{r} + \frac{C}{rp^{\frac{1}{\gamma}}}\frac{\partial p}{\partial \theta} = 0$$

A stochastic triggering disturbance could appear in several ways:

-- Introduction through reacting, mixing flow-field condition

-- An intermittent blockage in propellant injector flow.

-- A sharp vibrational, translational, or rotational engine acceleration.

Develop accurate and efficient computational models of unstable combustion and flow in LPRE chamber. Develop stochastic methods for predicting probability of an instability. Identify triggering mechanisms.

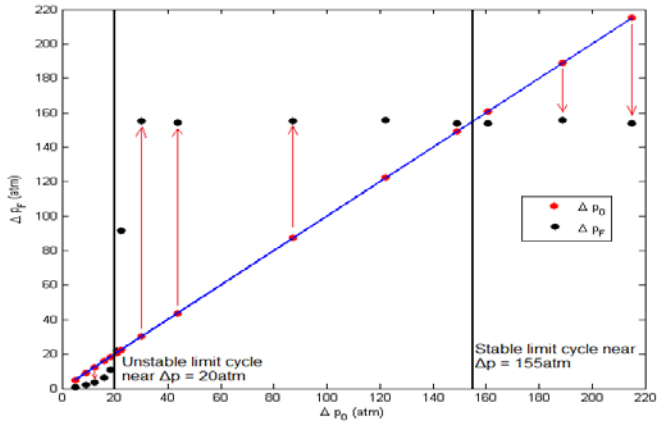

Ten-coaxial-injector Simulation -- A turbulent jet diffusion flame at each injector.
Time lag from mixing and kinetics.
-- Similar results with oscillating dipole disturbance, directed Gaussian pulse, body force, injector pulse.

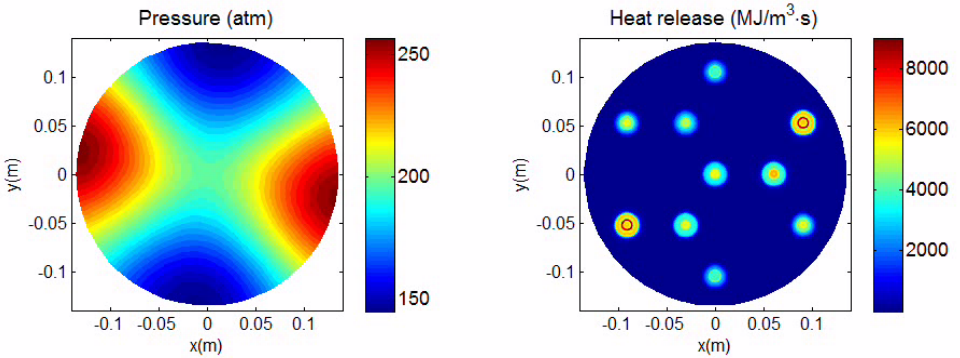

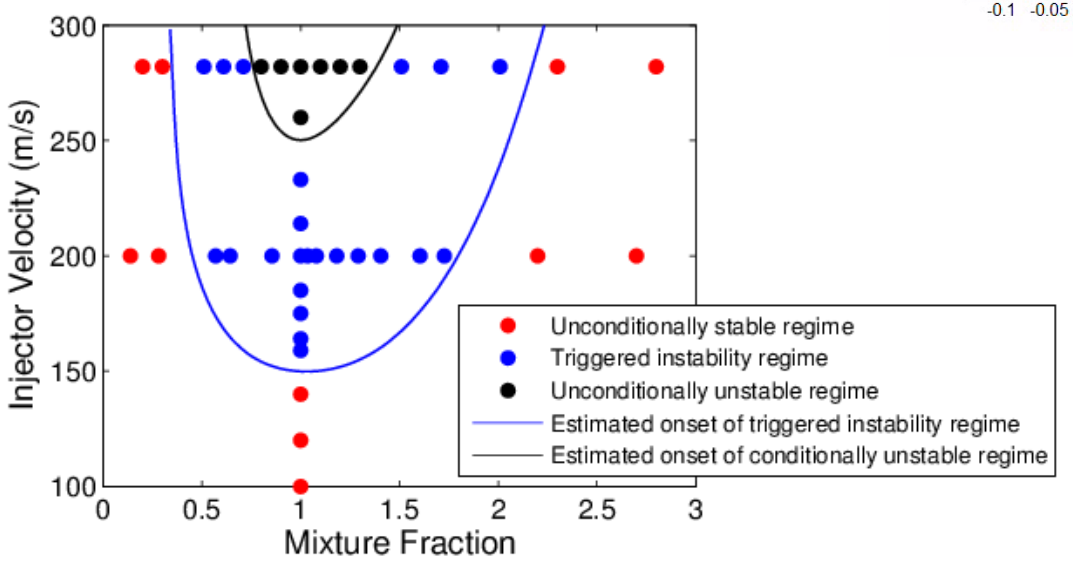

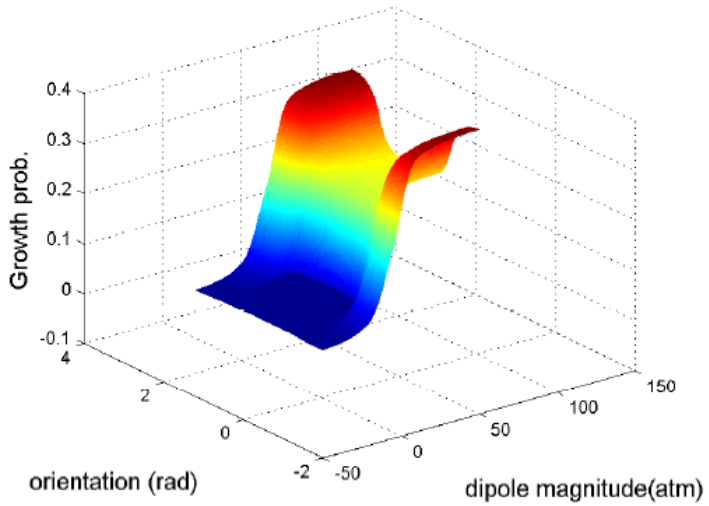

Stochastic Analysis of Triggering Mechanism

Polynomial Chaos Expansion (PCE) Method

The several characteristics of the disturbing pulse will be the random variables (RV) and form the vector ξ.

-- Equations for wave dynamics governing pressure and velocity.

$$\mathcal{L}_1(\mathbf{n}, r, \theta, t, \boldsymbol{\xi}) = \mathbf{f}_1(r, \theta, t, \mathbf{m}, \boldsymbol{\xi})$$

-- Diffusion/advection/reaction equations for each injector governing temperature and mass fractions.

$$\mathcal{L}_2(\mathbf{m}, x, \eta, t, \boldsymbol{\xi}) = \mathbf{f}_2(x, \eta, t, \mathbf{n}, \boldsymbol{\xi})$$

-- Expand the dependent variables in a series of Legendre polynomials (PCE)

$$\mathbf{n}(r, \theta, t, \boldsymbol{\xi}) \approx \sum_{k=0}^{P} \mathbf{n}_k(r, \theta, t)\, \Psi_k(\boldsymbol{\xi})$$

$$\mathbf{m}(x, \eta, t, \boldsymbol{\xi}) \approx \sum_{k=0}^{P} \mathbf{m}_k(x, \eta, t)\, \Psi_k(\boldsymbol{\xi})$$

-- Truncate to "converge" the series.

***P+1 = (n+ l)! /(n! l!)*, *l* is degree of polynomial, *n* is number of RV.**

-- Substitute PCE in equations and solve resulting PDEs for coefficients by finite-differences.

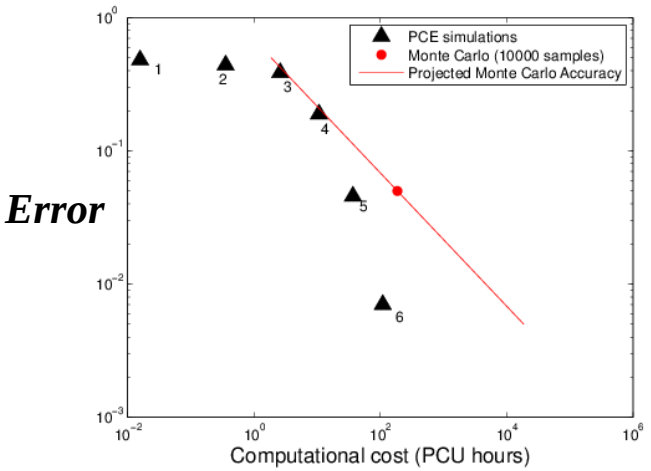

Quantitative Error vs. Computational Cost -- Better than Monte Carlo

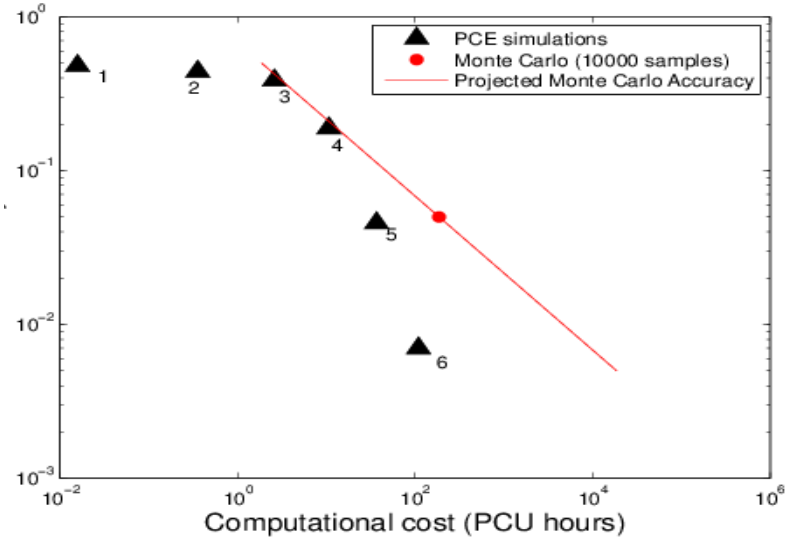

For triggering of spinning (standing) wave, pulsing duration matching an odd (any) multiple of chamber half (full) period is optimal.

Marginal Probability

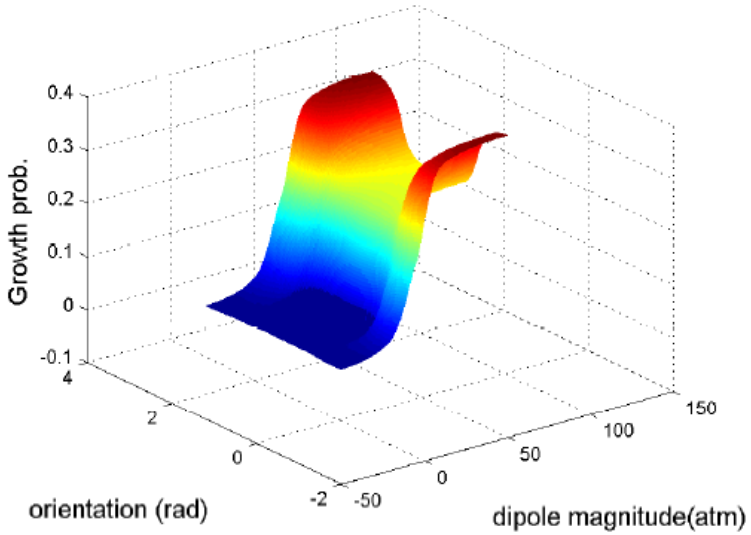

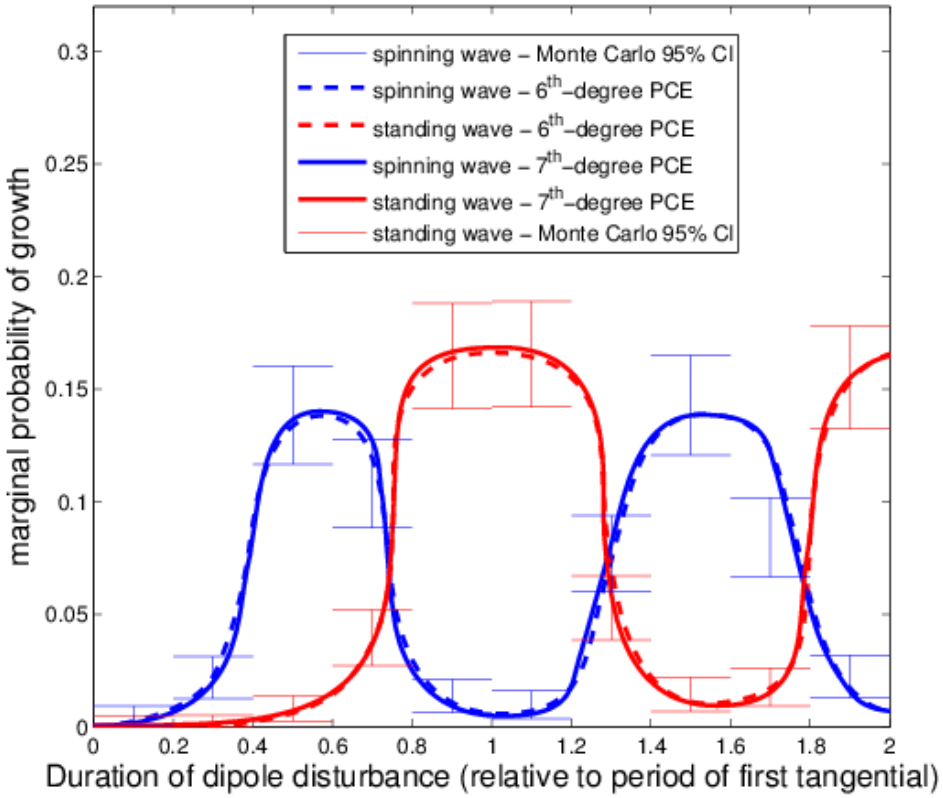

New Physics for Triggering: Engine Acceleration or Vibration -- Stochastic Simulation

- **Applied acceleration influences the probability of triggering with either linear motion or elliptical-path motion.**
- **Maximal conditional probability of growth occurs when acceleration has the first transverse mode frequency.**
- **For considerable departures from $2000Hz$, probability of growth decreases significantly.**
- **Even for a mismatched frequency, probability of growth is non-zero, due to the unconditionally unstable portion of the parameter space.**
- **Probability of growth to a limit cycle increases monotonically with increasing acceleration amplitude.**

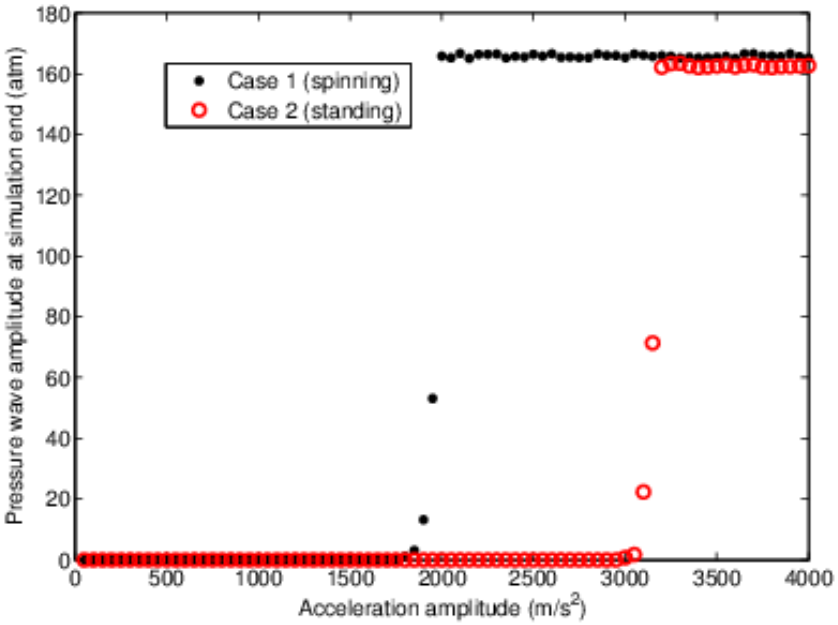

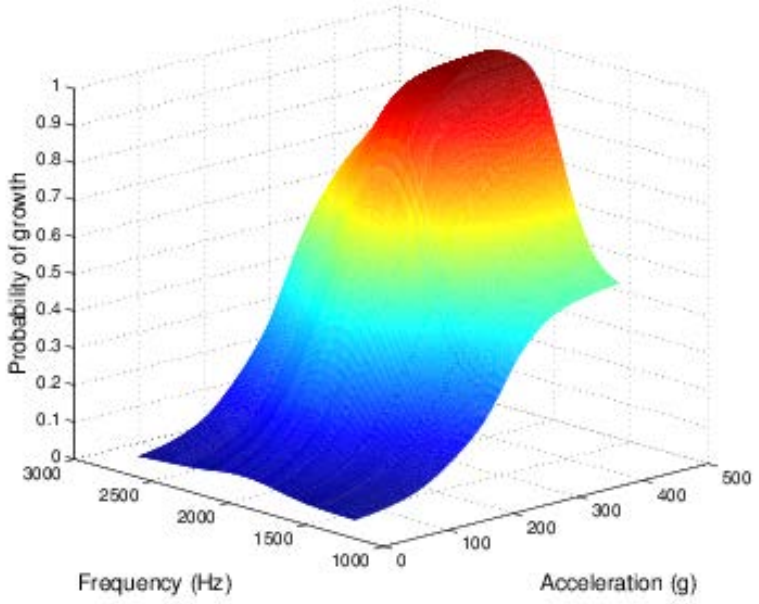

Anti-Pulses as Control Mechanisms

The same mechanisms that cause an instability can be applied, with proper magnitude and timing, to arrest a growing instability. This can work for disruptive combustion event, applied acceleration, or injector blockage. Clearly, strong potential for a control mechanism exists through this use of "anti-pulsing."

- **When the delay to the second pulse is larger than $5\tau_F/2$, an out-of-phase second pulse will reduce the instability's magnitude temporarily, but the instability will continue its growth to a limit cycle**
- **Two "anti-pulses", however, may cause a decay of the instability if they occur in close succession**

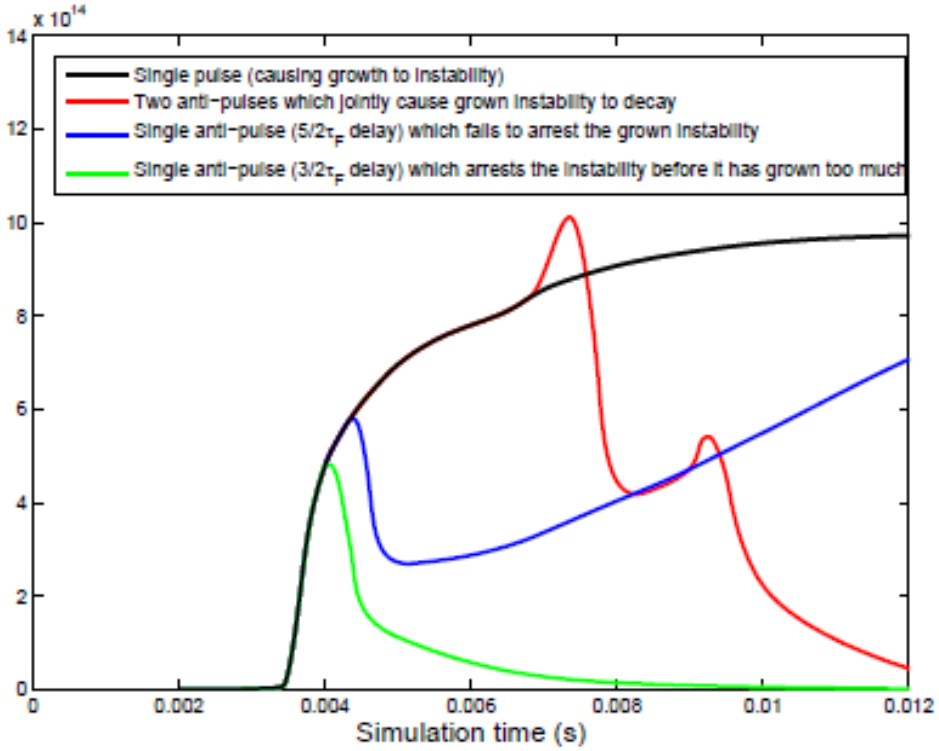

Two-time variable asymptotic analysis determines the slow time behavior of amplitude and phase by eliminating third-order nonlinear resonance. $\sigma = M = \varepsilon^2.$

Two first-order ODEs describe the transient behavior and yield a limit cycle.

$$\frac{dA}{d\tau} = k_1 A + k_2 A^3 \quad ; \quad \frac{d\psi}{d\tau} = -2\omega_2 - k_3 - k_4 A^2$$

$$A = A* \equiv \sqrt{-k_1/k_2} \qquad \omega_2 = -(k_3 + k_4 A*^2)/2.$$

$$\frac{A(\tau)}{A_0} = \left[(1 + \frac{k_2}{k_1} A_0^2) e^{-2k_1\tau} - \frac{k_2}{k_1} A_0^2\right]^{-1/2} = \left[(1 - (\frac{A_0}{A*})^2) e^{-2k_1\tau} + (\frac{A_0}{A*})^2\right]^{-1/2}$$

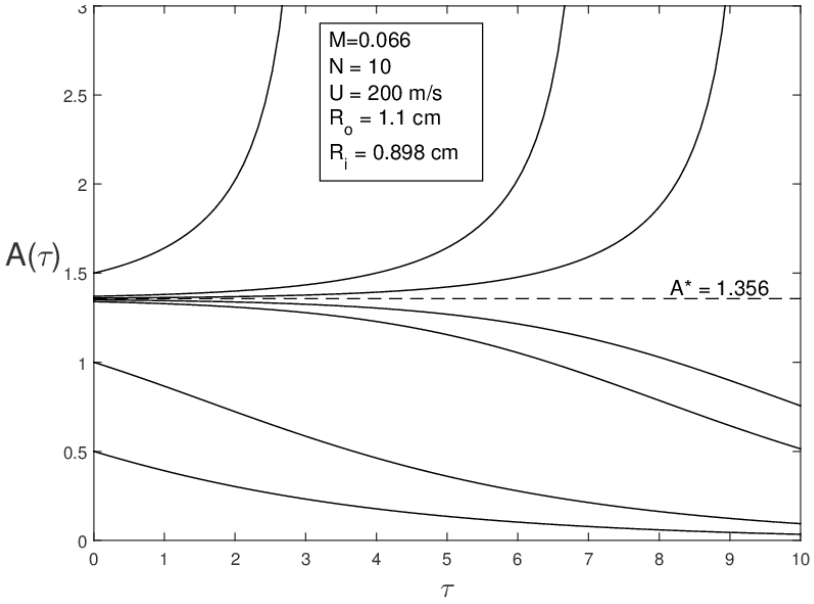

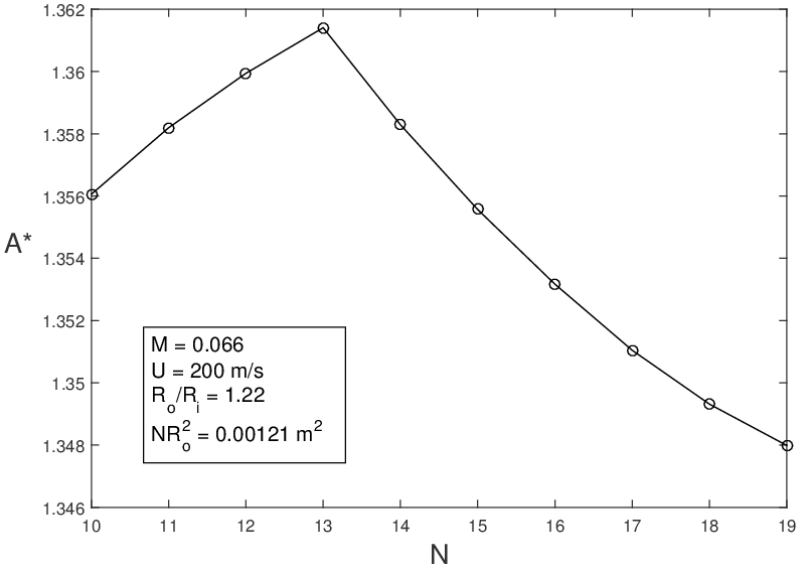

Experimental Verification with Purdue Rectangular Engine with Transverse Oscillations.

There is good agreement with experiment. Acoustic instability is predicted in all cases with 5 − 8% under-prediction of limit-cycle amplitude and frequency. Greatest relative errors are observed in the most stable cases where simulation predicts linear stability, with a very small instability threshold.

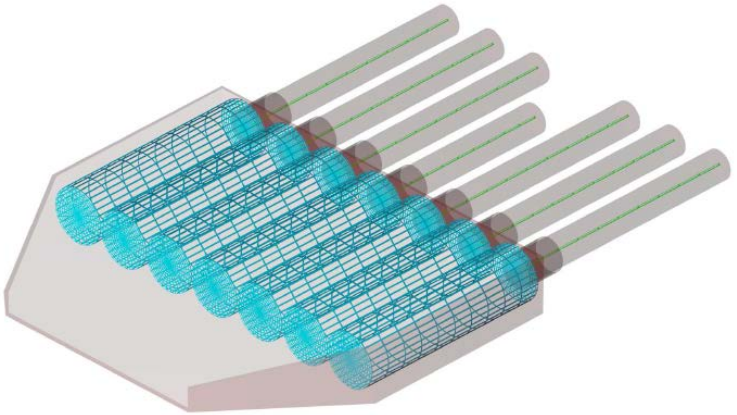

Test Case	simulation limit-cycle ampl. (kPa)	expt. limit-cycle ampl. (kPa)	simulation freq. (Hz)	expt. freq. (Hz)	relative errors (ampl. / freq.)
OOXOXOO	580	620	1931	2032	6%/5%
OXXOXXO	398	415	1720	1807	4%/5%
XOOOOOX	161	175	1766	1855	8%/5%
XOXOXOX	65	70	1803	1912	7%/6%

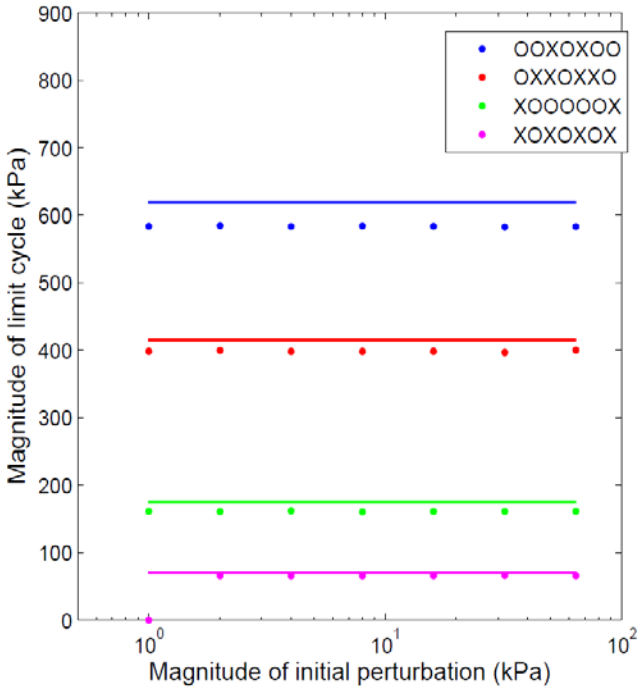

Single Injector Engine – Longitudinal Mode Instability: Continuously Variable Resonance Combustor (CVRC)

Second experimental iteration

- **Gaseous methane fuel (T= 300 K)**
- **Decomposed H_2O_2**
- **Axial fuel injection**
- **Oxidizer post length varies**
- **Different stability domains**
- **Ideal for numerical simulations**
- **P_{mean}= 1400 kPa**

Reactants	T_{cr} (K)	P_{cr} (atm)
CH_4	190.6	45.6
O_2	154.6	49.8
H_2	33.2	12.8
H_2O	647	217.75
CO_2	304.18	72.83
CO	134.45	34.98

High-fidelity hybrid RANS/LES or purely LES simulations of CVRC

- **3D: Harvazinski (2012), Harvazinski et al. (2012), Garby et al. (2013), Srinivasan et al. (2014)**
- **Axisymmetric: Harvazinski (2012), Garby et al. (2013), Sardeshmukh et al. (2015)**
- **Good agreement with experiments: 3D with global mechanism or axisymmetric with detailed mechanism**
- **Computationally expensive**

Simulation Details

- CH4 at T = 300 K, $\dot{m}_f = 0.027\ kg/s$
- 58 % H2O & 42 % O2 at T= 1030 K, $\dot{m}_o = 0.027\ kg/s$
- Choked nozzle: $\mathrm{M}_{x,ex} = 0.12$
- 38-cm chamber length
- 3 different cases: 9-cm, 12-cm, 14-cm ox. Post
- Benchmark against: experimental data (Yu et al., 2012), 3D simulations (Srinivasan et al.)

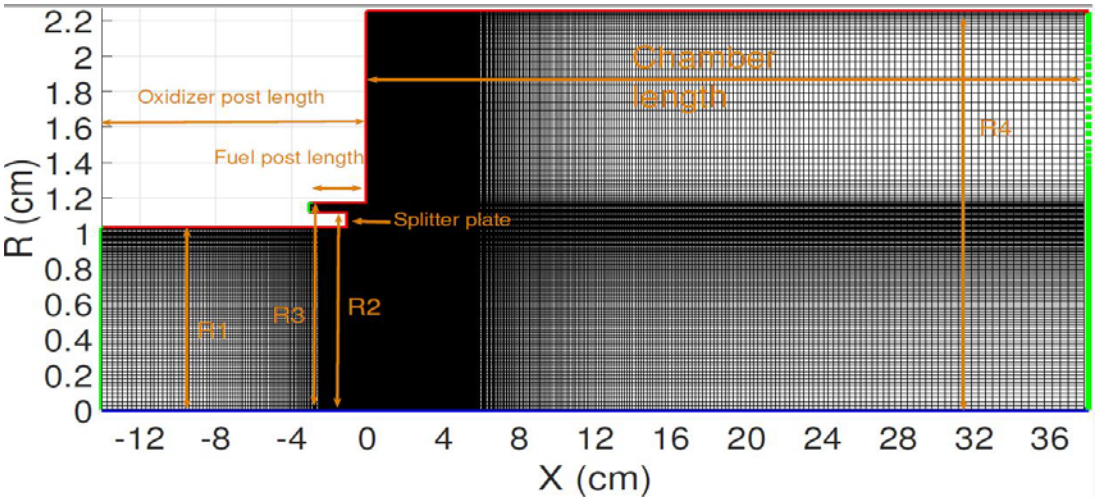

Combustion Model

$$\frac{\partial \bar{\rho}\tilde{E}}{\partial t} + \frac{\partial \tilde{v}_j(\bar{\rho}\tilde{E} + \bar{p})}{\partial x_j} = \overbrace{\dot{\tilde{\omega}}_T}^{\text{Heat Release Rate}}, \qquad \frac{\partial \bar{\rho}\tilde{Y}_L}{\partial t} + \frac{\partial \tilde{v}_j \bar{\rho}\tilde{Y}_L}{\partial x_j} = \overbrace{\dot{\tilde{\omega}}_L}^{\text{species reaction rate}}.$$

$$\dot{\tilde{\omega}}_f = -A\tilde{T}^b exp\left(\frac{E_a}{R\tilde{T}}\right)\tilde{X}_f^m \tilde{X}_o^n, \quad \dot{\tilde{\omega}}_T = \sum_L^N \dot{\tilde{\omega}}_L \overbrace{\Delta h^o_{f,L}}^{\text{Heat of formation}}, \quad \tilde{X}_L = \frac{W}{W_L}\tilde{Y}_L$$

$$\frac{\partial \bar{\rho}\tilde{Z}}{\partial t} + \frac{\partial \bar{\rho}\tilde{v}_j\tilde{Z}}{\partial x_j} = \frac{\partial}{\partial x_j}\left[\left(\frac{\lambda}{c_p} + \frac{\mu_t}{Sc_t}\right)\frac{\partial \tilde{Z}}{\partial x_j}\right]$$

$$\frac{\partial \bar{\rho}\widetilde{Z^2}}{\partial t} + \frac{\partial \bar{\rho}\tilde{v}_j\widetilde{Z^2}}{\partial x_j} = \frac{\partial}{\partial x_j}\left[\left(\frac{\lambda}{c_p} + \frac{\mu_t}{Sc_t}\right)\frac{\partial \widetilde{Z^2}}{\partial x_j}\right] - \bar{\rho}C_x\omega(\widetilde{Z^2} - \tilde{Z}^2)$$

$$\frac{\partial \bar{\rho}\tilde{C}}{\partial t} + \frac{\partial \bar{\rho}\tilde{v}_j\tilde{C}}{\partial x_j} = \frac{\partial}{\partial x_j}\left[\left(\frac{\lambda}{c_p} + \frac{\mu_t}{Sc_t}\right)\frac{\partial \tilde{C}}{\partial x_j}\right] + \dot{\tilde{\omega}}_C$$

Flamelet Model

- **Compressible Flamelet Progress Variable**
  - **Chemical time scales < turbulent time scales**
  - **Non-premixed counterflow diffusion flame**

$$-\frac{\rho\chi}{2}\frac{\partial^2\psi_i}{\partial Z^2} = \dot{\omega}_i, \qquad \overbrace{Z}^{\text{Mixture Fraction}} = \frac{\overbrace{Y_f}^{\text{Fuel mass fraction}}}{Y_f + \underbrace{Y_o}_{\text{Ox. mass fraction}}}$$

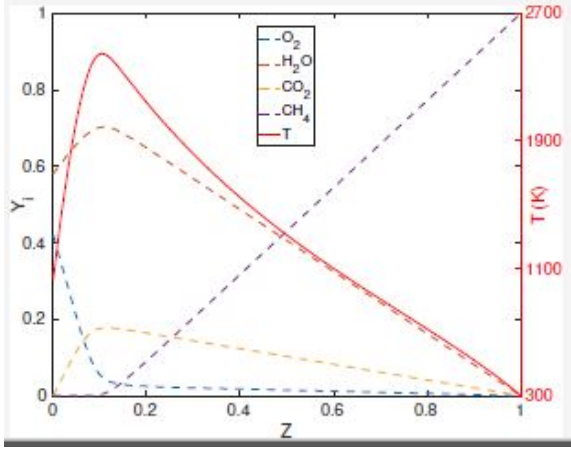

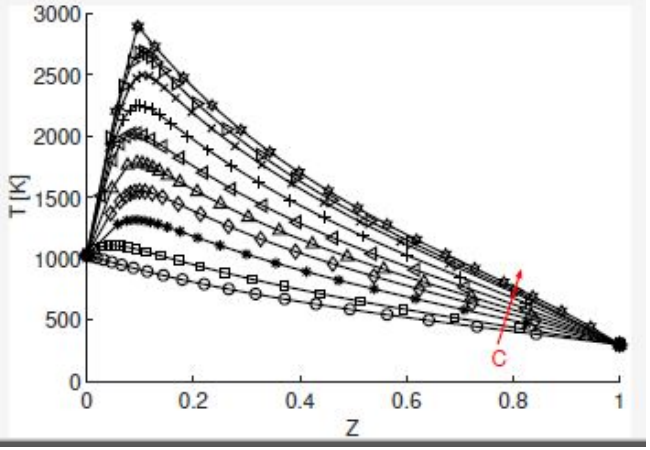

Vortex structures synchronized with oscillations and influencing combustion process

- **The choked nozzle case simulates the Purdue CVRC with 14 cm Ox port.**
- **The open-end case maintain the same mass flux, mixture ratio and pressure but allows no combustion instability.**
- **The oscillations significantly affect vortex formation, mixing, and combustion.**
- **Vortex frequency increases matching oscillation frequency.**

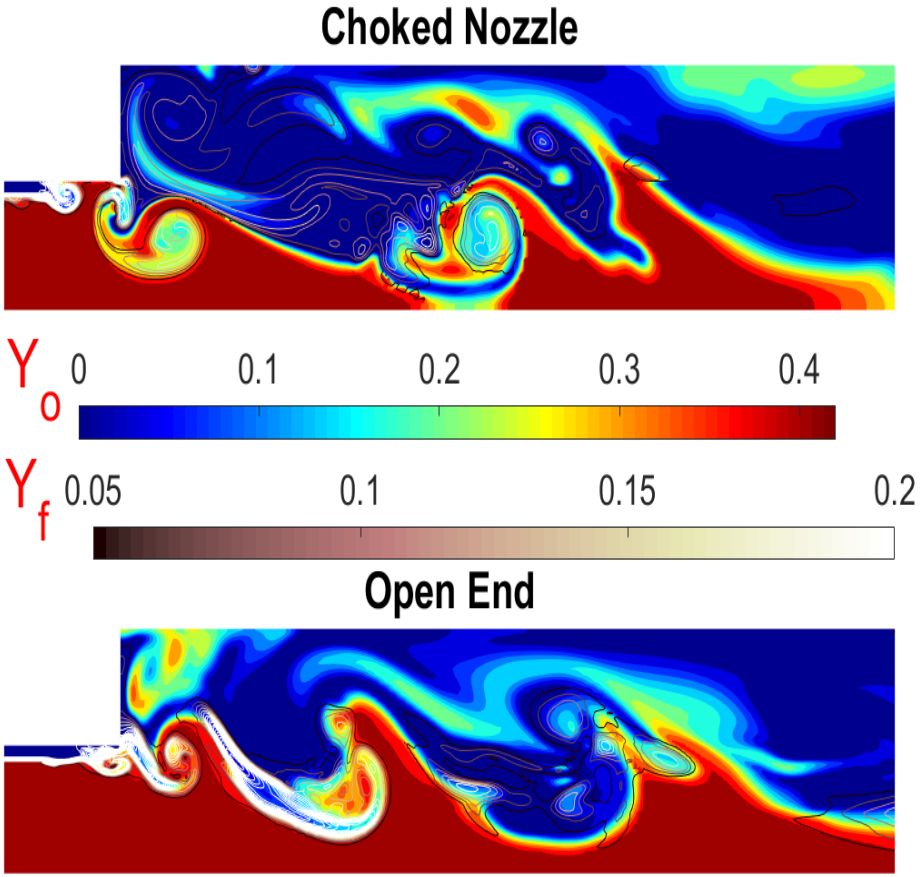

Coupling of Acoustics and Vorticity

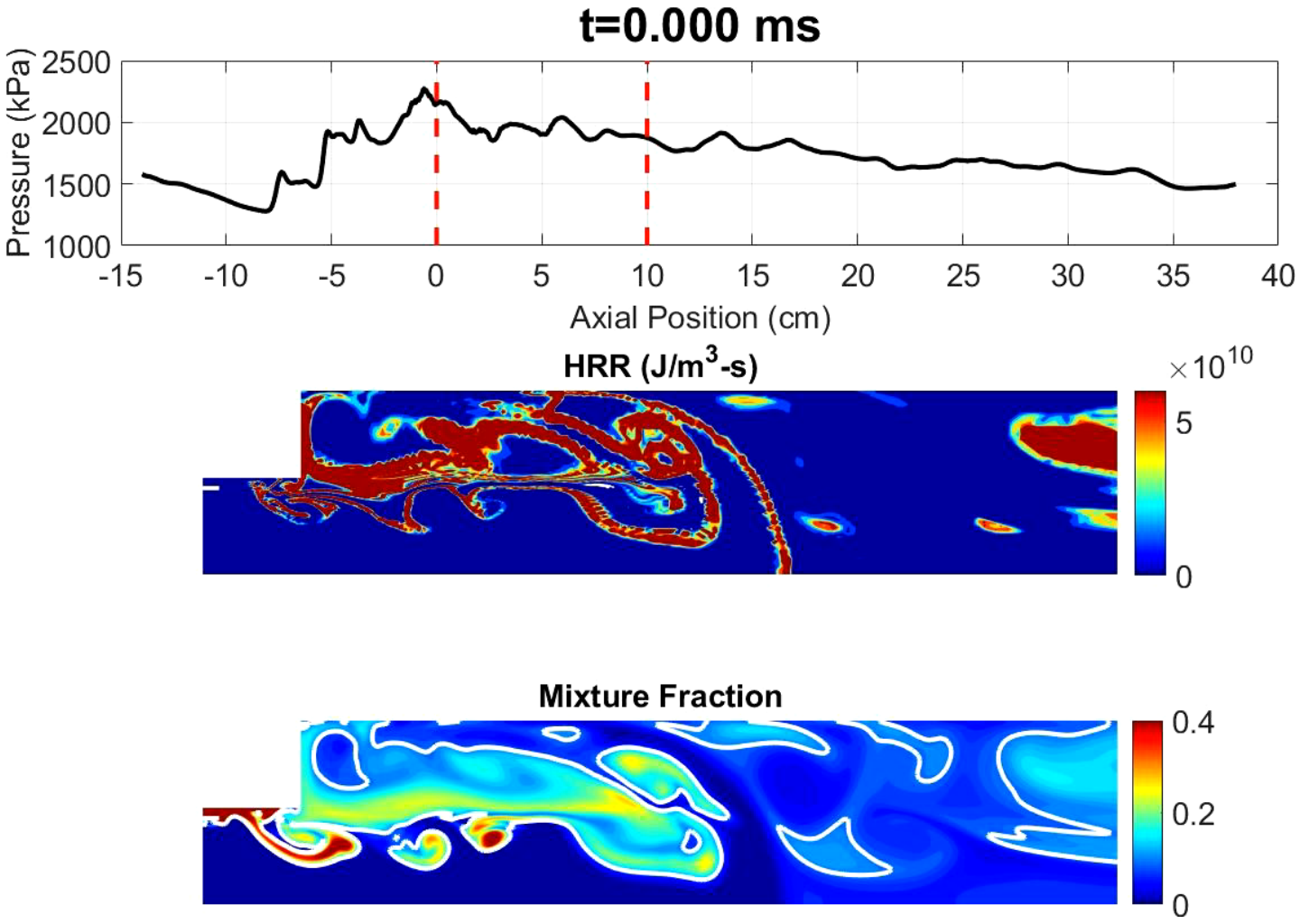

Power Spectral Density

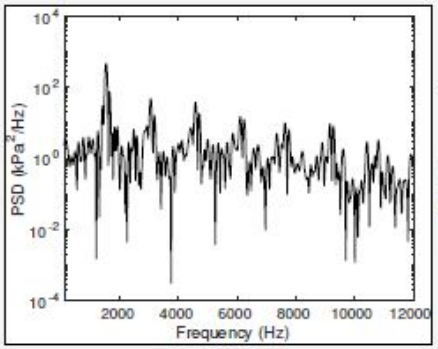

psd analysis

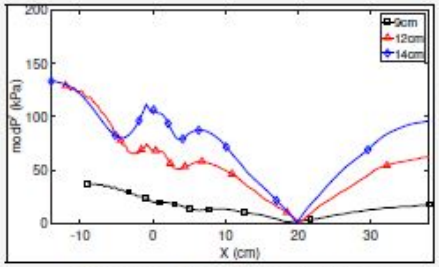

Current computation

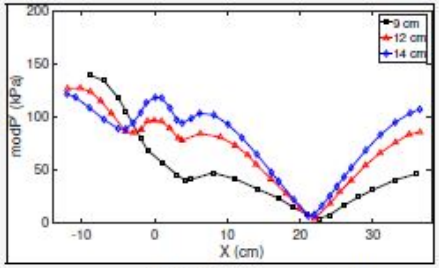

Srinivasan et al.

Ox. Post Length	1st mode (Hz)	2nd mode (Hz)	3rd Mode (Hz)
9 cm - Computation (UCI)	1400	2900	4350
9 cm - Computation (Srinivasan)	1686	2791	3373
9 cm - Experiment	1392	2704	3772
12 cm - Computation (UCI)	1600	2906	4500
12 cm - Computation (Srinivasan)	1613	3268	4881
12 cm - Experiment	1385	2777	4169
14 cm - Computation (UCI)	1520	2880	4440
14 cm - Computation (Srinivasan)	1592	3130	4722
14 cm - Experiment	1331	2655	3986

Institution	Type	Mesh size	Number of species	Core hours per ms
UCI	Axisymmetric	6.26E4	27	0.28
CNRS[1]	Axisymmetric	7E5	5	160
Purdue University	Axisymmetric	5.5E4	4	53
Purdue University	Axisymmetric	2E5	4	480
CNRS	3D	14E6	5	1024
AFRL[2]	3D	4E6	4	11520
AFRL	3D	4E6	31	259200
Georgia Tech.	3D	1.4E6	5	3333

Triggering

- Two different wave types
- Two durations: two and four periods
- T_{wall}= 1030 K, 1800 K

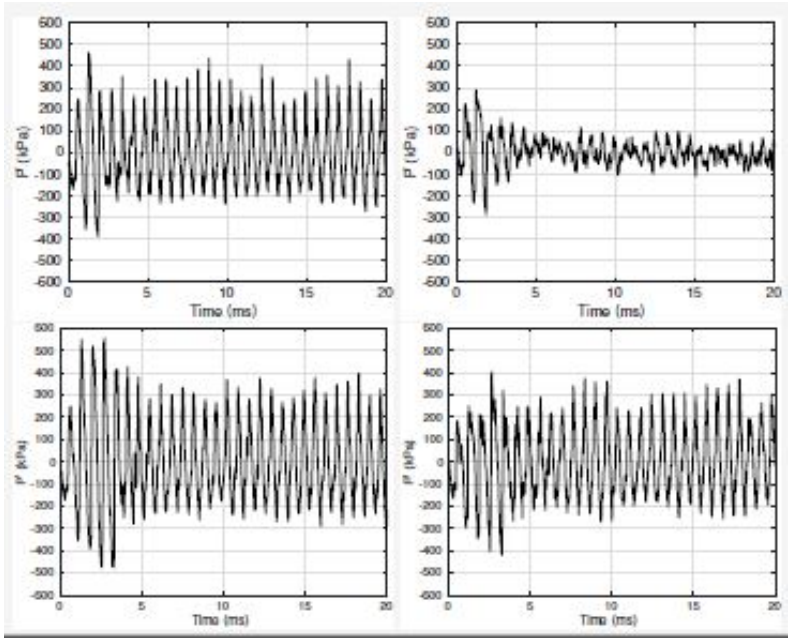

$$m = m_i\left(1 + \epsilon \sum_{i=1}^{n} A_i sin(\omega_i t)\right)$$

$$\epsilon = 0.75$$

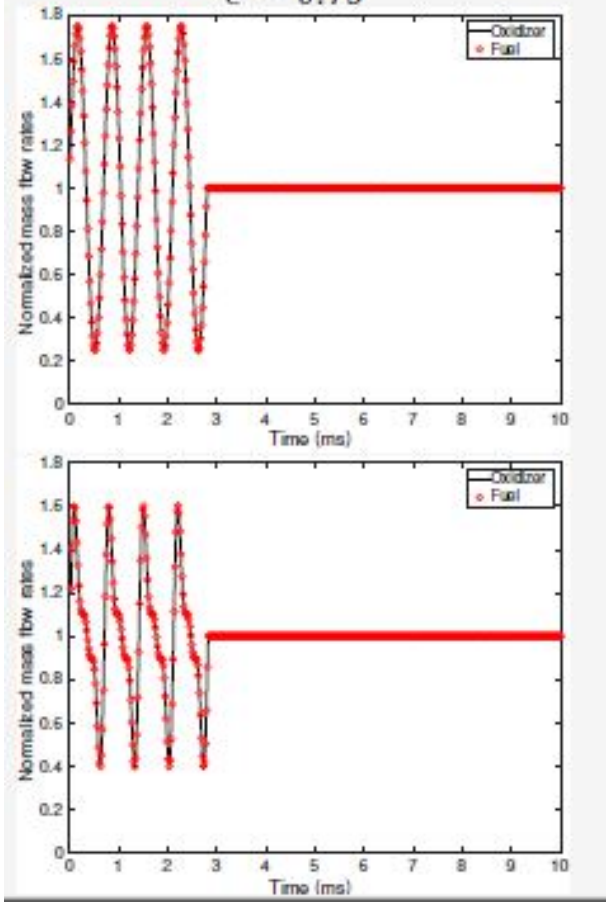

Effect of Mass Flux Perturbation

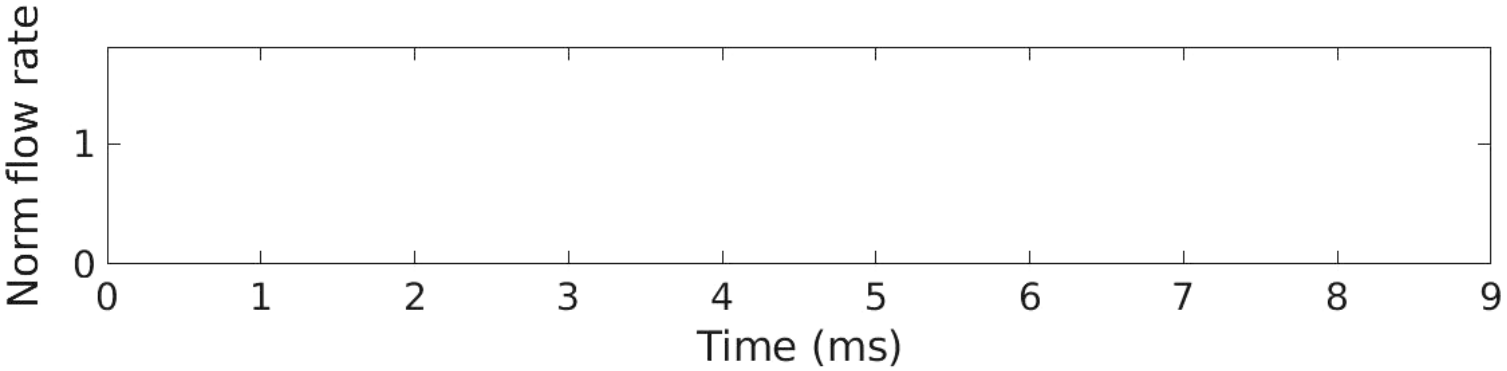

Perturbed

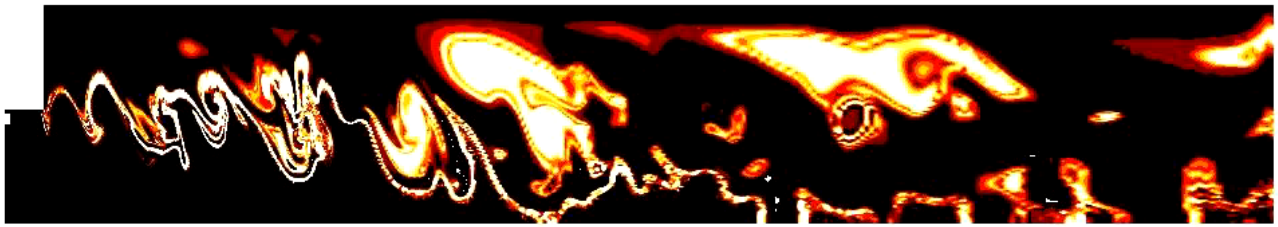

Unperturbed

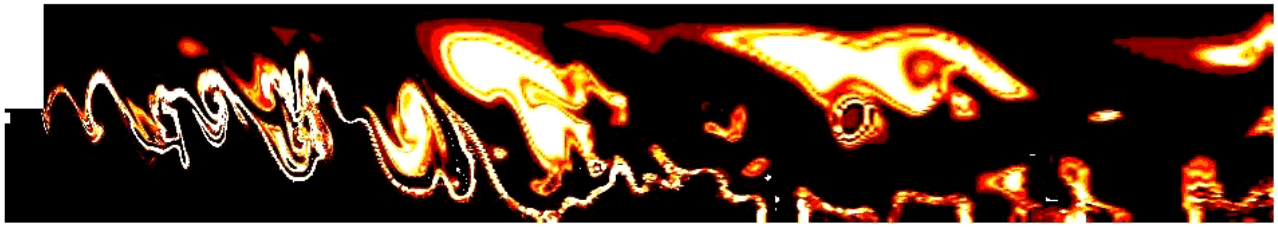

Multi-injector Computations

3D hybrid LES-RANS resolving vortex structures

Couplings with choked nozzle and co-axial injector ports

Methane-oxygen one-step kinetics

(Flamelet model planned for the future)

10, 19, and 30 injectors are examined.

Nineteen-injector case is portrayed here.

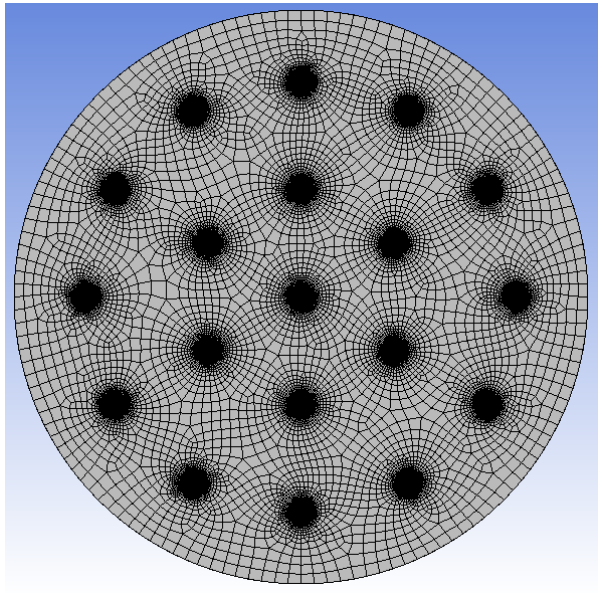

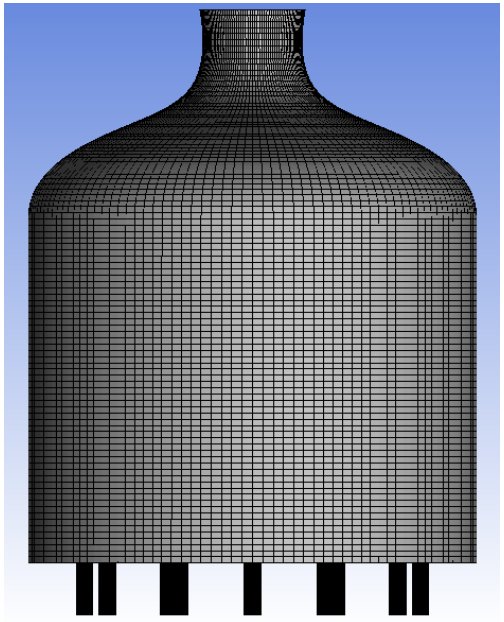

Cases Studied for 10 and 19 Injectors

Table 1. Test Cases Parameters

	Injectors	D_c (cm)	D_t (cm)	$\dot{m}$ (kg/s)	ϵ	instability mode	f (Hz)	T_a (K)	η_{CH4}
$10A$	10	28	9.5	80	0	none	-	3398.8	80.0%
$10B$	10	28	8.2	65	0	spontaneous longitudinal	1455.1	3539.5	86.55%
$10C$	10	28	6.7	49	0	spontaneous longitudinal	1596.3	3813	97.2%
$19A$	19	28	9.5	80	0	spontaneous longitudinal	1595.3	3916	84.5%
$19B$	19	28	9.5	80	1.0	spontaneous longitudinal	1622.7	3866.3	80%
$19LA$	19	43	9.5	80	0	spontaneous longitudinal	1437	3434.5	86%
$19LB$	19	43	9.5	80	0.25	triggered longitudinal	1448	3505	88.5%
$19LC$	19	43	9.5	80	0.50	triggered tangential	1771.4	4151	95.3%
$19LD$	19	43	9.5	80	0.75	triggered tangential	1796.5	4215	95.4%
$19LE$	19	43	9.5	80	1.0	triggered tangential	1807.5	4352	95.5%
$19LF$	19	43	9.5	80	1.0	triggered tangential	1803.5	4080	94.5%

Spontaneous Longitudinal Mode
19 injectors - 28 cm diameter

Pressure

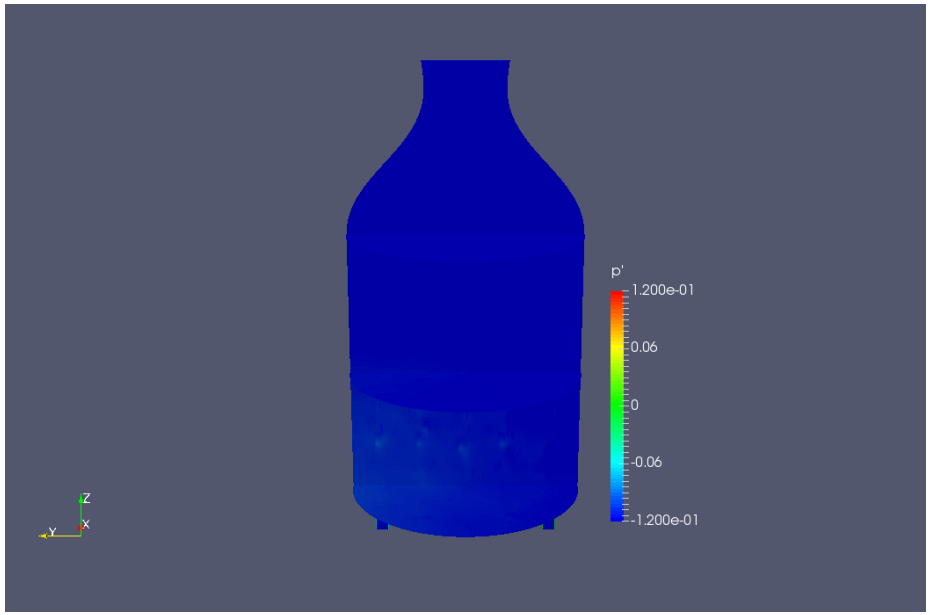

Heat Release Rate

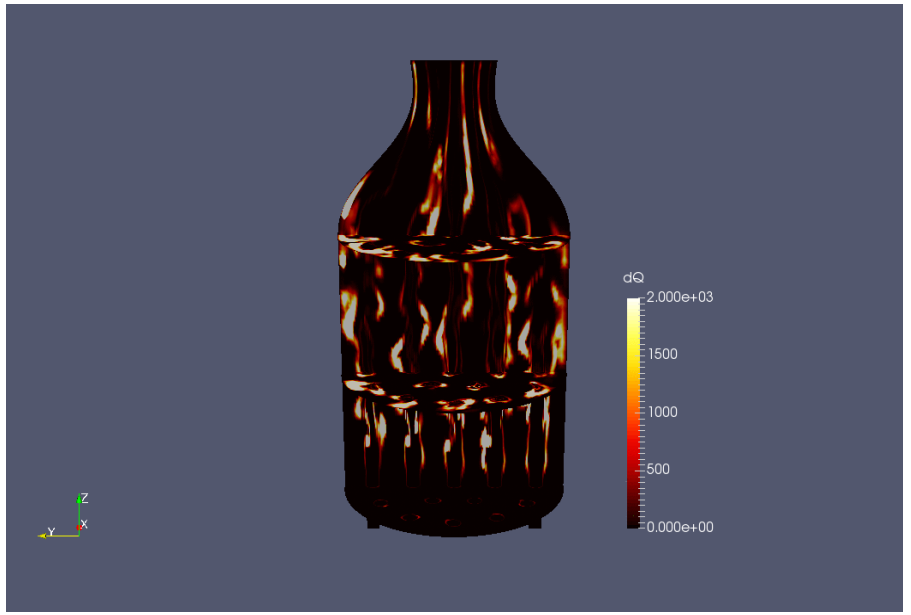

Triggered Tangential Mode
19 injectors - 43 cm diameter
Different triggering for spinning and standing modes

Spinning Wave -- Location of red and blue injectors rotate with out-of-phase pulses for a few cycles

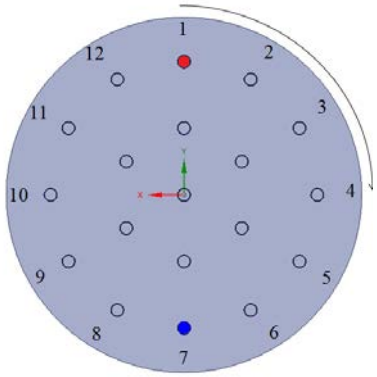

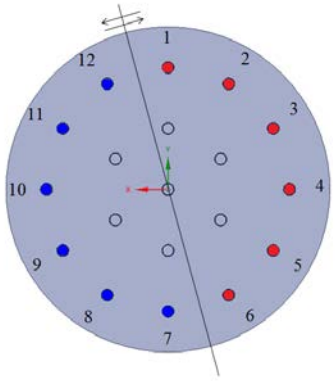

Standing Wave -- Red and blue injectors pulse out of phase for a few cycles

Pressure

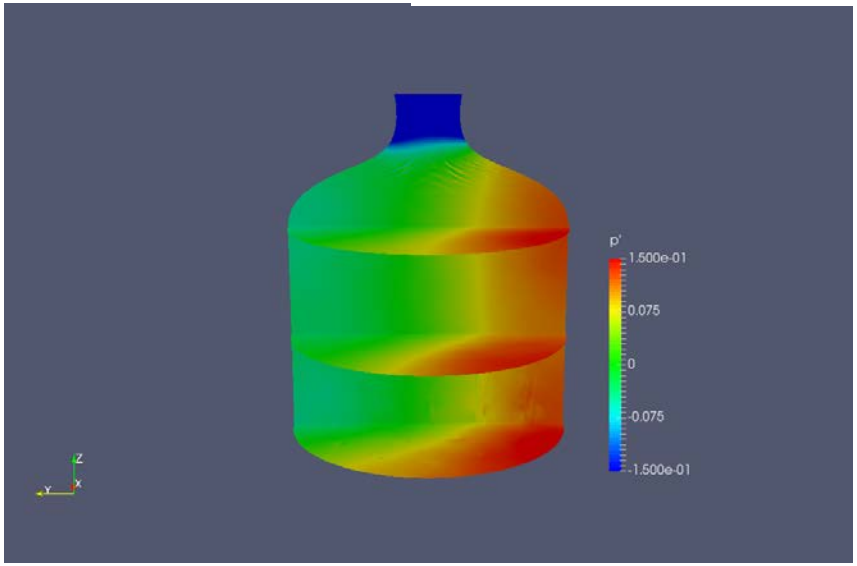

Heat release rate

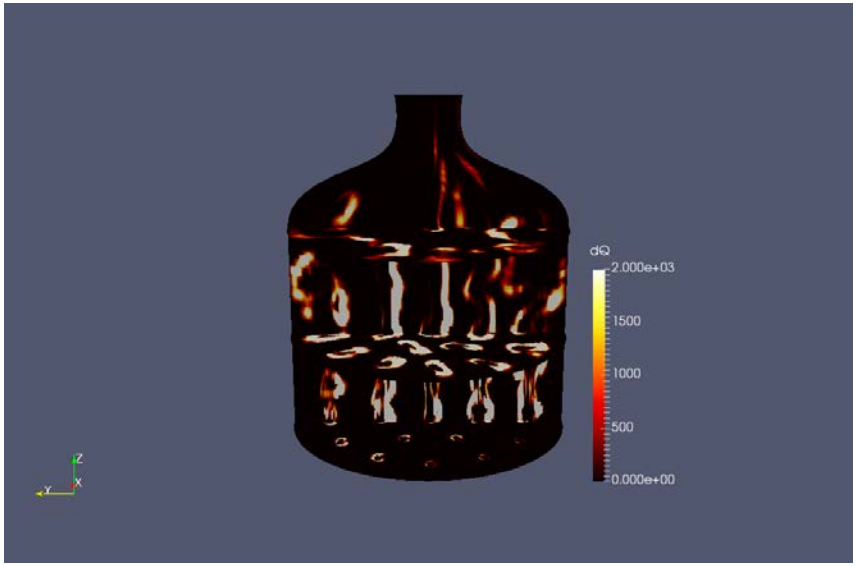

Rayleigh Index
Tangential Spinning Mode
19 Injectors

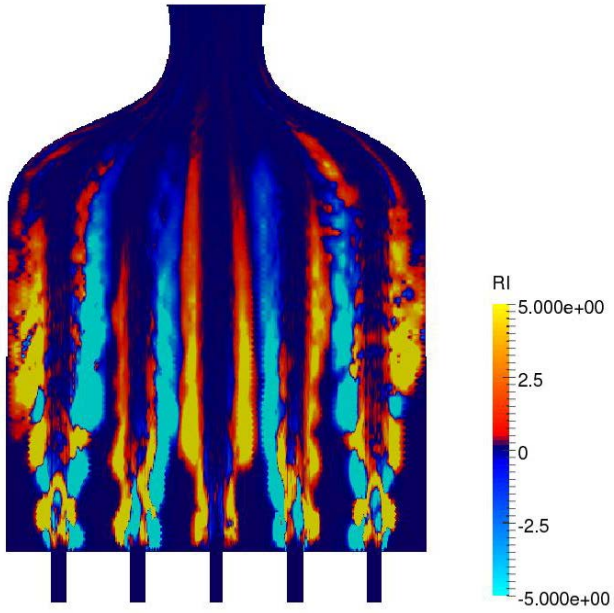

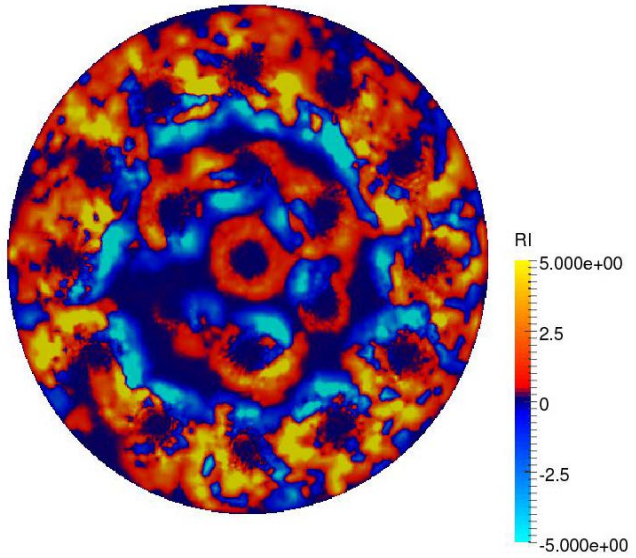

Phasing of Heat Release Rate and Vorticity

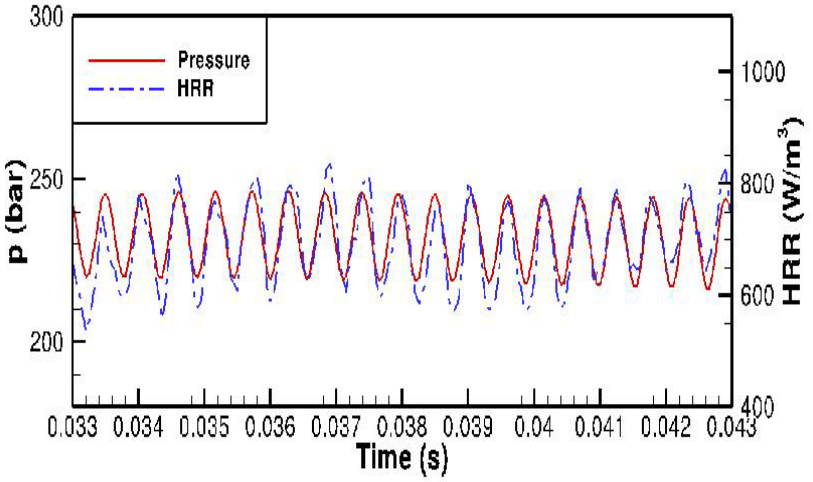

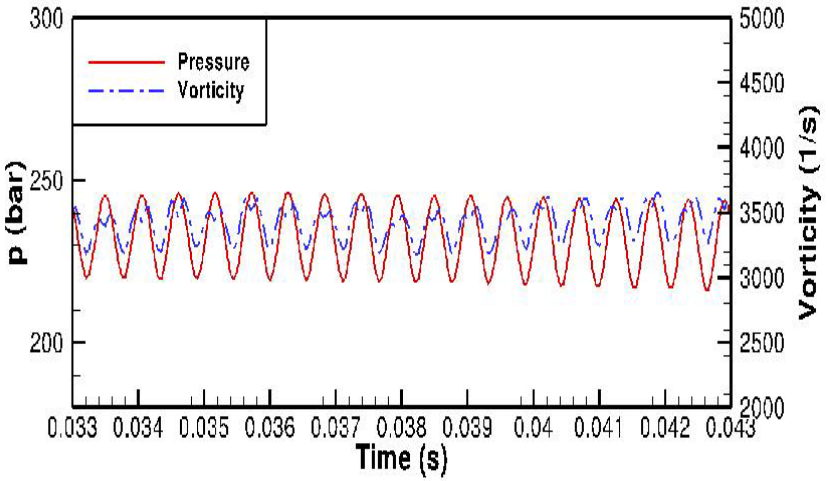

Pressure Contour at Quarter Period Intervals

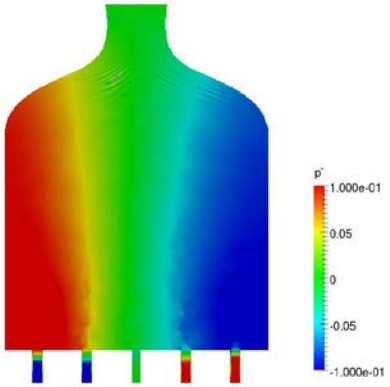

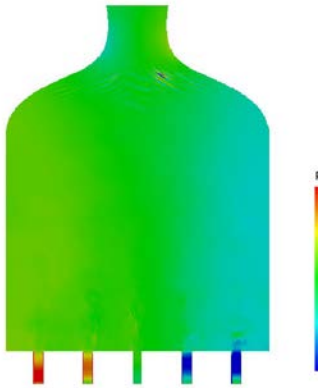

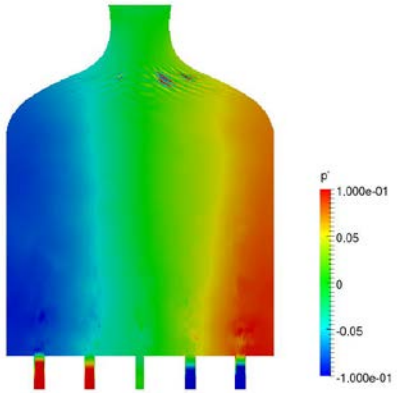

Helicity

Dot Product of Velocity and Vorticity

An Indicator of Streamwise Vorticity

The acoustically driven transverse flow in the combustion chamber shears the axial jet flow and initiates internal circulation in the transverse plane of jet flow

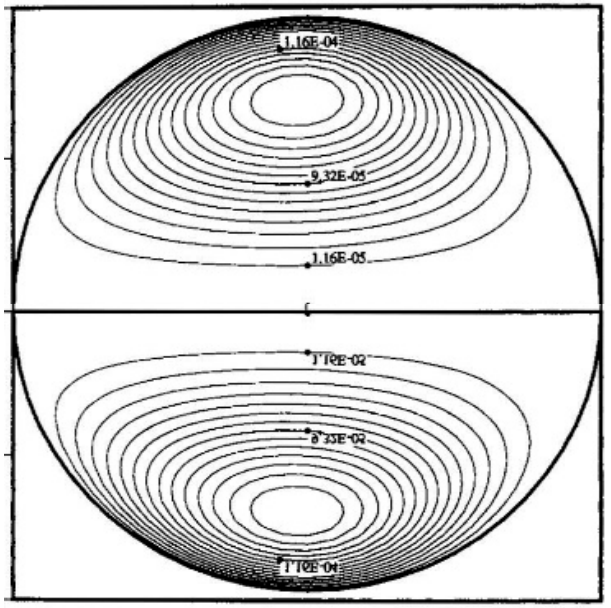

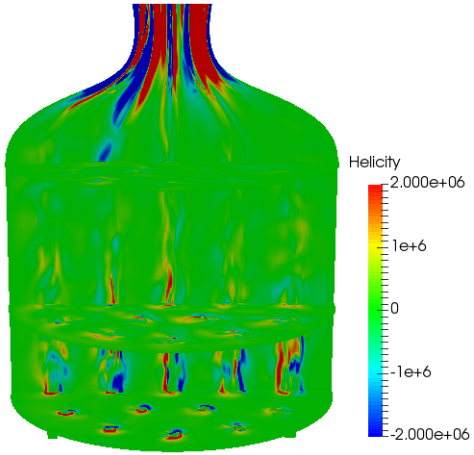

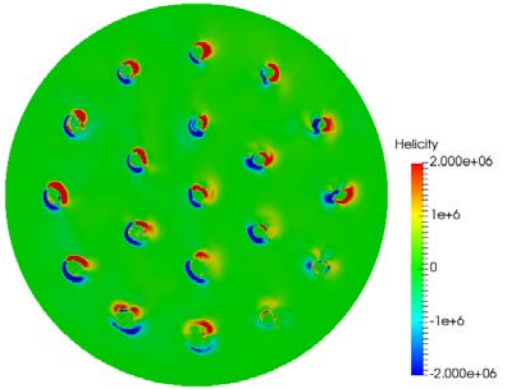

The streamwise counter-rotating vortices should enhance mixing and burning.

Table 1. Combustion chamber parameters

	$D_{chamber}$ (cm)	D_{ox} (mm)	D_{fuel} (mm)	$L_{chamber}$ (cm)	Mixture Ratio(ox/fuel)	Chamber pressure	T_{ox} (K)	T_{fuel} (K)	D_{throat} (cm)
19-inj	28 or 43	14.2	16.1	33	4:1	230bar	400	400	9.5
30-inj	14.376	7.64	9.10	24.2	2.55:1	130bar	119.8	281	8.4

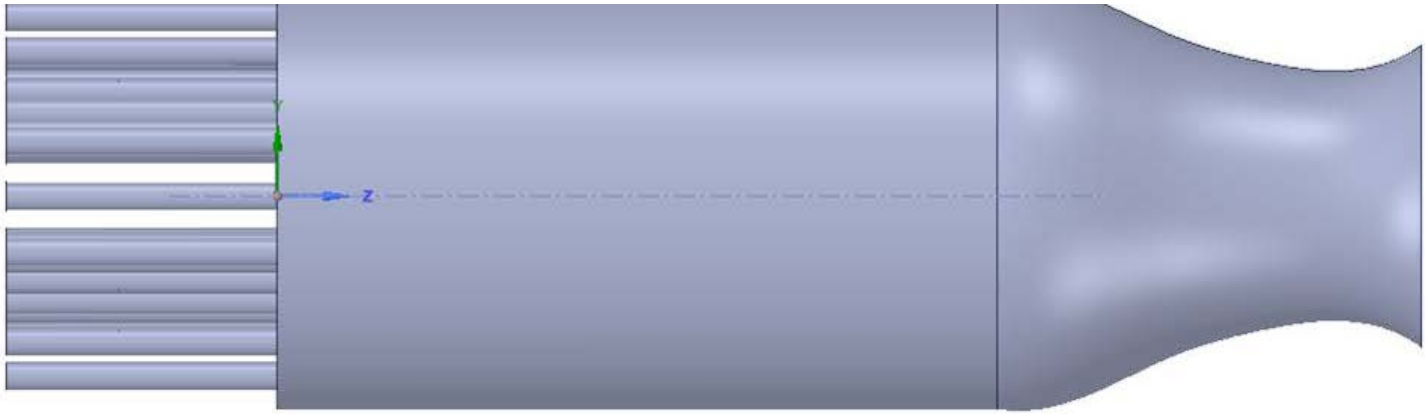

An Attempt is made to match radial and tangential mass-flow distribution with the 82-injector experiment of Jensen et al. (1989)

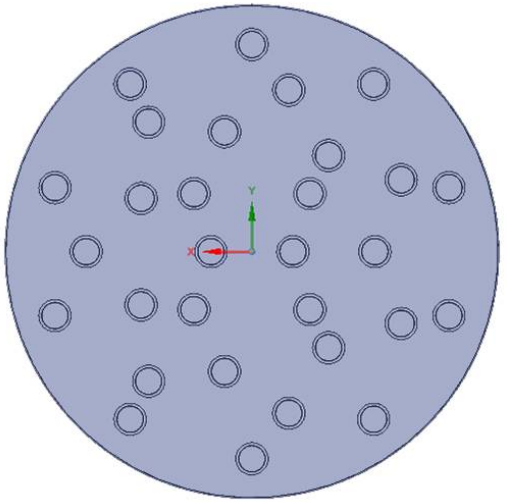

REAL-GAS EFFECTS ON COMPRESSIBLE FLOW

Comparison with Ideal-gas Results

-- Reductions in mass flux, momentum flux, and thrust for flow through choked nozzle at fixed chamber pressure. CO_2, 30 MPa, 1000 K.

-- Increased pressure amplitude for piston-driven oscillations. CO_2, 30 MPa, 1000 K.

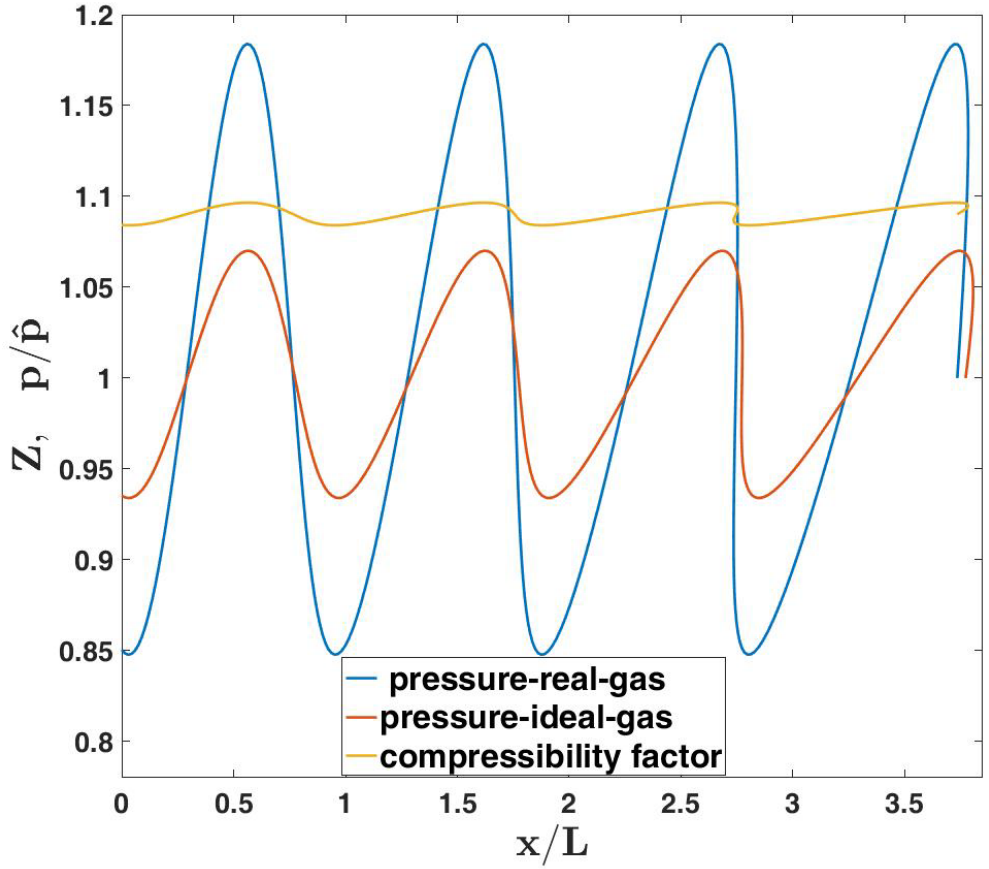

Summary of Advances

- **Reduced-order modeling (ROM)**
  - **-- Reduced dimension**
  - **-- Hybrid LES-RANS**
  - **-- Flamelet model for combustion**
  - **-- Perturbation analysis**
- **Stochastic analysis**
- **Comparison with experiments**
- **New physical insights**
  - **-- New triggering mechanism – acceleration / vibration**
  - **-- Trigger low-amplitude oscillations to higher-amplitude limit cycle**
  - **-- Potential control mechanisms**
  - **-- Role of vorticity dynamics**
  - **-- Real-gas capabilities**

Thank You.

3D Representation of marginal probability

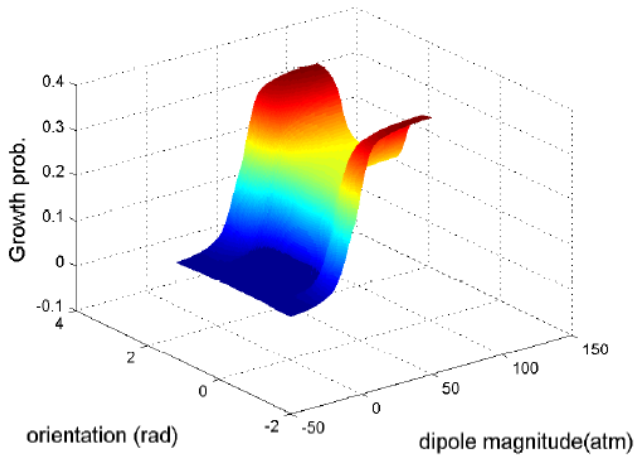

A disturbance at a larger radial position or with a better matching oscillation period is more likely to cause instability.

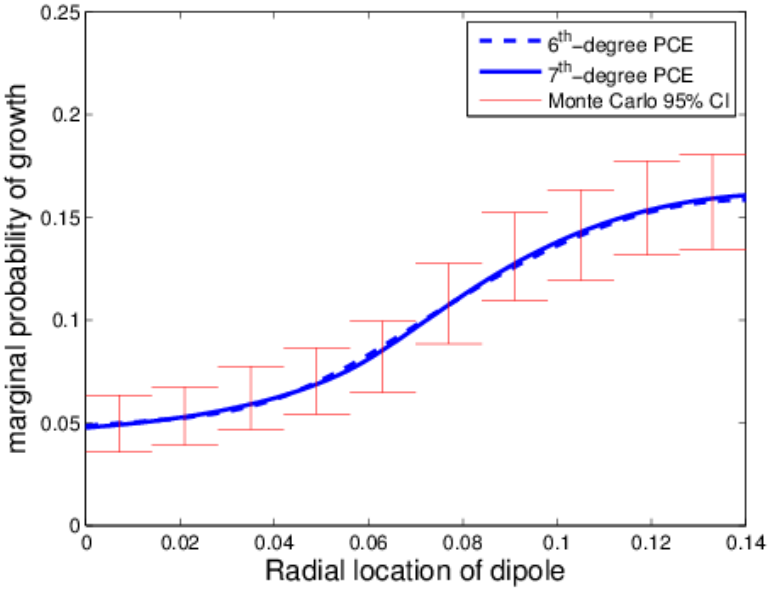

For triggering of spinning (standing) wave, pulsing duration matching an odd (any) multiple of chamber half (full) period is optimal.

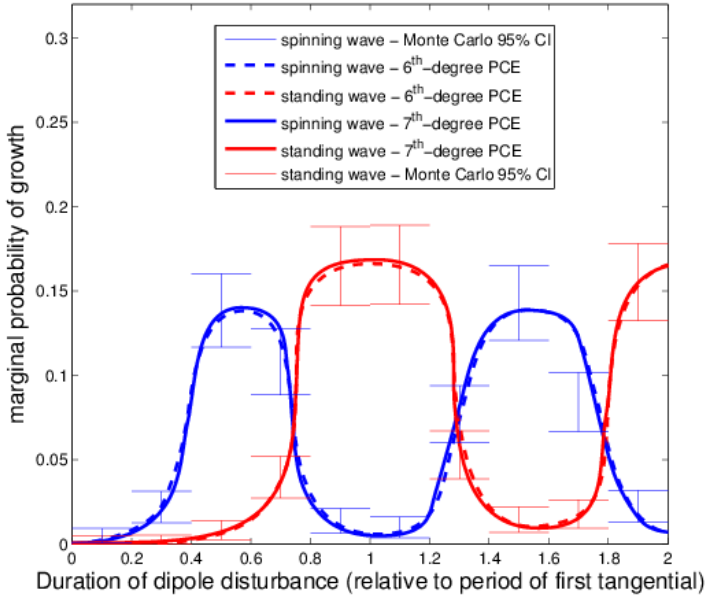

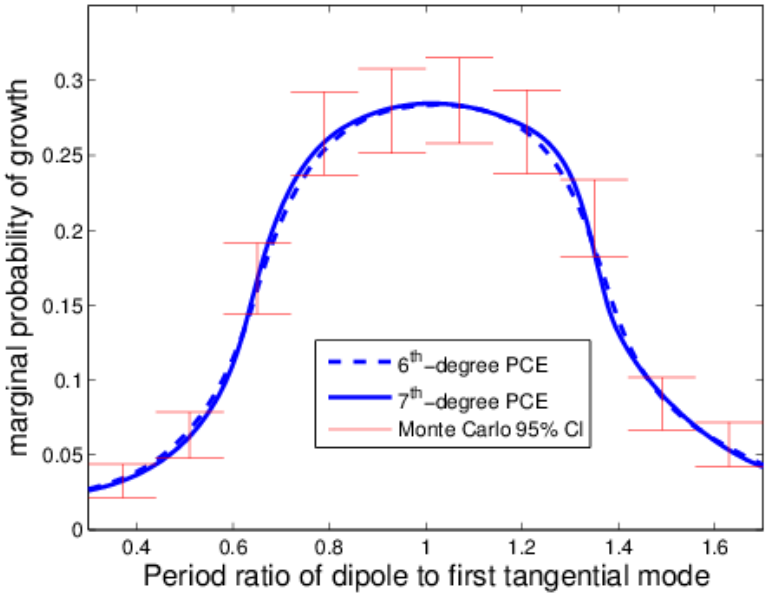

Pressure Signal Comparisons

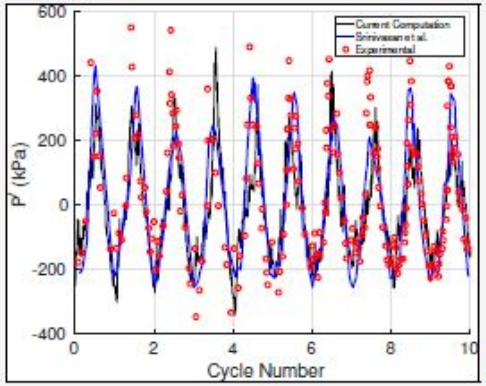

12-cm case

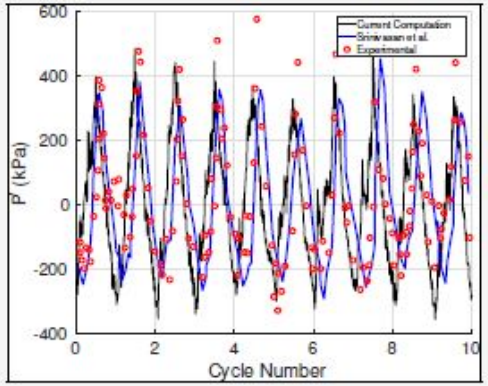

14-cm case

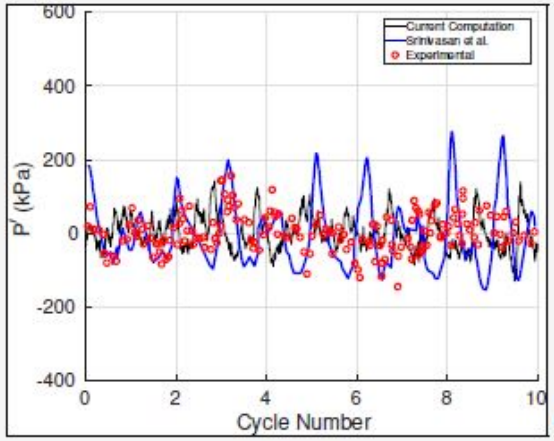

9-cm case

Comp

Main Flow Equations

- Fully conserved, Favre-averaged Navier-Stokes equation

$$\frac{\partial \bar{\rho}}{\partial t} + \frac{\partial \bar{\rho}\tilde{v}_j}{\partial x_j} = 0$$

$$\frac{\partial \bar{\rho}\tilde{v}_j}{\partial t} + \frac{\partial \bar{\rho}\tilde{v}_i\tilde{v}_j}{\partial x_j} = -\frac{\partial \bar{p}}{\partial x_i} + \frac{\partial(\tau_{ij}+\tau_{ij}^R)}{\partial x_j}$$

$$\frac{\partial \bar{\rho}\tilde{E}}{\partial t} + \frac{\partial \tilde{v}_j(\bar{\rho}\tilde{E}+\bar{p})}{\partial x_j} = \frac{\partial}{\partial x_j}\left[\tilde{v}_i(\tau_{ij}+\tau_{ij}^R) + \left(\mu + \sigma_k \mu_t \frac{\partial k}{\partial x_j}\right)\right] + \frac{\partial}{\partial x_j}\left[\left(\frac{\lambda}{c_p} + \frac{\mu_t}{Pr_t}\right)\frac{\partial \tilde{h}}{\partial x j}\right]$$

Total energy

$$\overbrace{\tilde{E}} = \underbrace{\frac{1}{2}\left(\sum_{j=1}^{n} v_j v_j\right)}_{\text{mean flow kinetic energy}} + \overbrace{k} + \tilde{e}, \qquad \underbrace{\tilde{e}}_{\text{thermal energy}} = \tilde{h} - \frac{\bar{p}}{\bar{\rho}}$$

T.K.E.

Heat of formation

$$\underbrace{\tilde{h}}_{\text{thermal enthalpy}} = \sum_{l=1}^{N} Y_l \left(\underbrace{h_{s,l}}_{\text{sensible enthalpy}} + \overbrace{\Delta h_{f,l}^o}\right), \qquad \underbrace{\bar{p} = \bar{\rho} R \tilde{T}}_{\text{Ideal gas law}}$$

Turbulence Model

- Delayed Detached Eddy Simulation
  - Based on the 2006 Wilcox k-ω two-equation RANS

$$\frac{\partial \bar{\rho} k}{\partial t} + \frac{\partial (\bar{\rho} \tilde{v}_j k)}{\partial x_j} = (\tau_{ij} + \tau_{ij}^R) \frac{\partial \tilde{v}_i}{\partial x_j} - \beta^* \bar{\rho} \omega k + \frac{\partial}{\partial x_j} \left[\left(\mu + \sigma_k \frac{\rho k}{\omega} \right) \frac{\partial k}{\partial x_j} \right]$$

$$\frac{\partial \bar{\rho} \omega}{\partial t} + \frac{\partial (\bar{\rho} \tilde{v}_j \omega)}{\partial x_j} = \frac{\gamma \omega}{k} (\tau_{ij} + \tau_{ij}^R) \frac{\partial \tilde{v}_i}{\partial x_j} - \beta \bar{\rho} \omega^2 + \frac{\partial}{\partial x_j} \left[\left(\mu + \sigma_\omega \frac{\bar{\rho} k}{\omega} \right) \frac{\partial \omega}{\partial x_j} \right] + \frac{\bar{\rho} \sigma_d}{\omega} \frac{\partial k}{\partial x_j} \frac{\partial \omega}{\partial x_j}$$

$$\mu_t = \frac{\bar{\rho} k}{\hat{\omega}}, \qquad \frac{\bar{\rho} k^{3/2}}{L_T^*} \simeq \beta^* \bar{\rho} \omega k, \qquad L_T^* = min(L_T, C_{DES} L_{GRID}),$$

$$L_T = \frac{k^{1/2}}{(\beta^* \omega)}, \quad L_{GRID} = L_T - F_D (L_T - \Delta), \quad F_D = 1 - tanh \left[\left(1.5 \frac{L_T}{d} \right)^3 \right]$$

ny

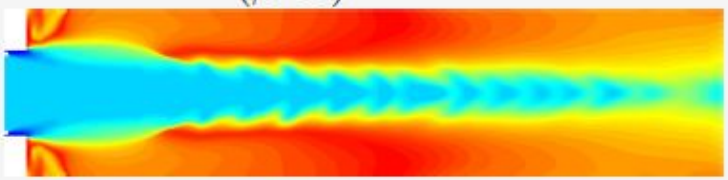

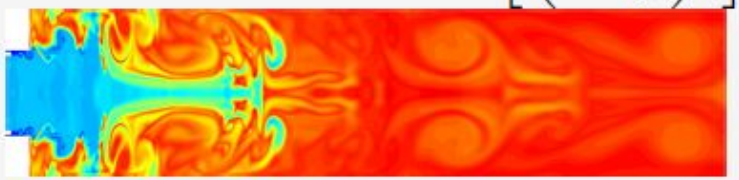

Real-gas effects on flame location and extinction

-- Counterflow diffusion flame location is modified from ideal-gas behavior because of density of colder gas even Though the flame region follows the ideal-gas law closely.

-- Extinction occurs at lower flame temperature and strain rate which is consequential for turbulent combustion.

-- Since temperature decreases at constant enthalpy and composition, a local minimum occurs in the extinction temperature as pressure increases.

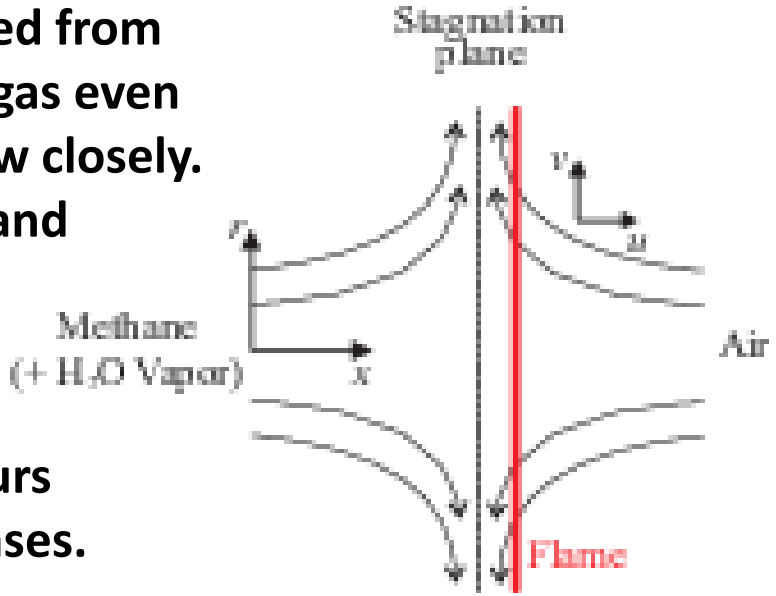

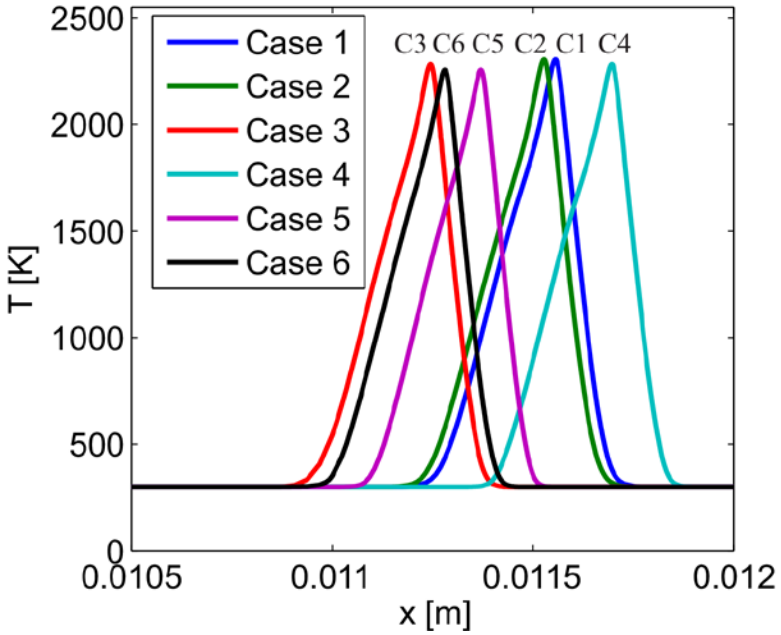

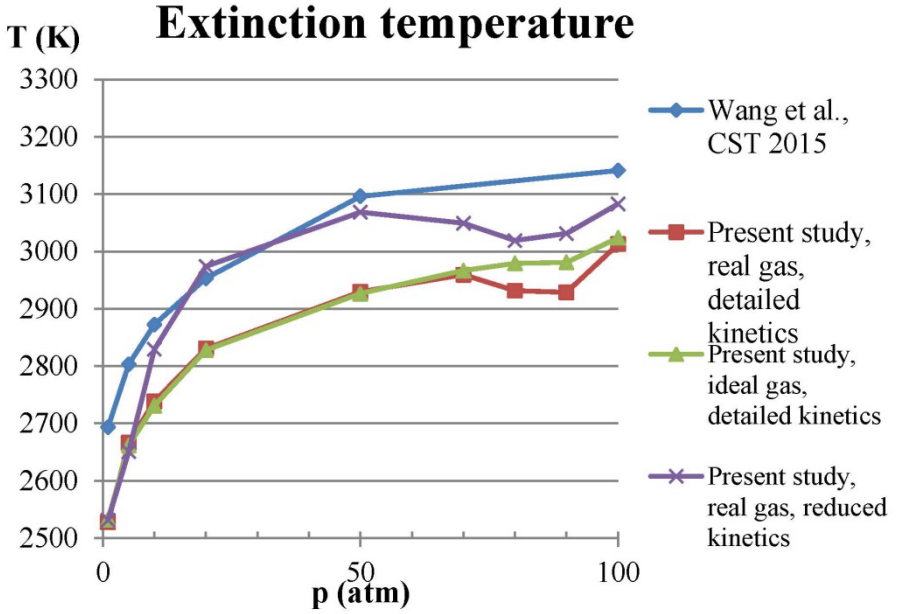

Computational Cost

Institution	Type	Mesh size	Number of species	Core hours per ms
UCI	Axisymmetric	6.26E4	27	0.28
CNRS[1]	Axisymmetric	7E5	5	160
Purdue University	Axisymmetric	5.5E4	4	53
Purdue University	Axisymmetric	2E5	4	480
CNRS	3D	14E6	5	1024
AFRL[2]	3D	4E6	4	11520
AFRL	3D	4E6	31	259200
Georgia Tech.	3D	1.4E6	5	3333

Stabilization

- Baseline case: 14-cm ox. Post with 38-cm chamber
- Six cases considered
- Isothermal wall: T= 1800 K, 1030 K, 600 K (adiabatic wall: 2700 K)

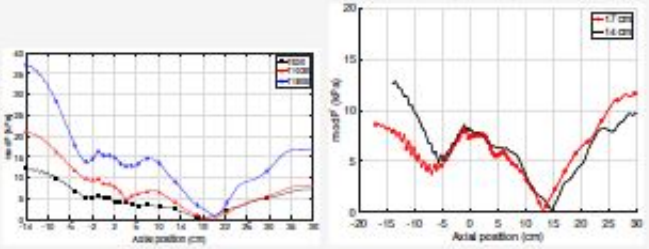

Isothermal cases Shortened chamber

Case	Configuration	Wall B.C.	f_1 (Hz)	Stable
1	14 & 38 cm	T – 1800 K	1422	No
2	14 & 38 cm	T – 1030 K	1397	No
3	14 & 38 cm	T – 600 K	1372	Yes
4	14 & 30 cm	Adiabatic	1771	Yes
5	17 & 30 cm	Adiabatic	1622	Yes
6	17 & 38 cm	Adiabatic	1447	No

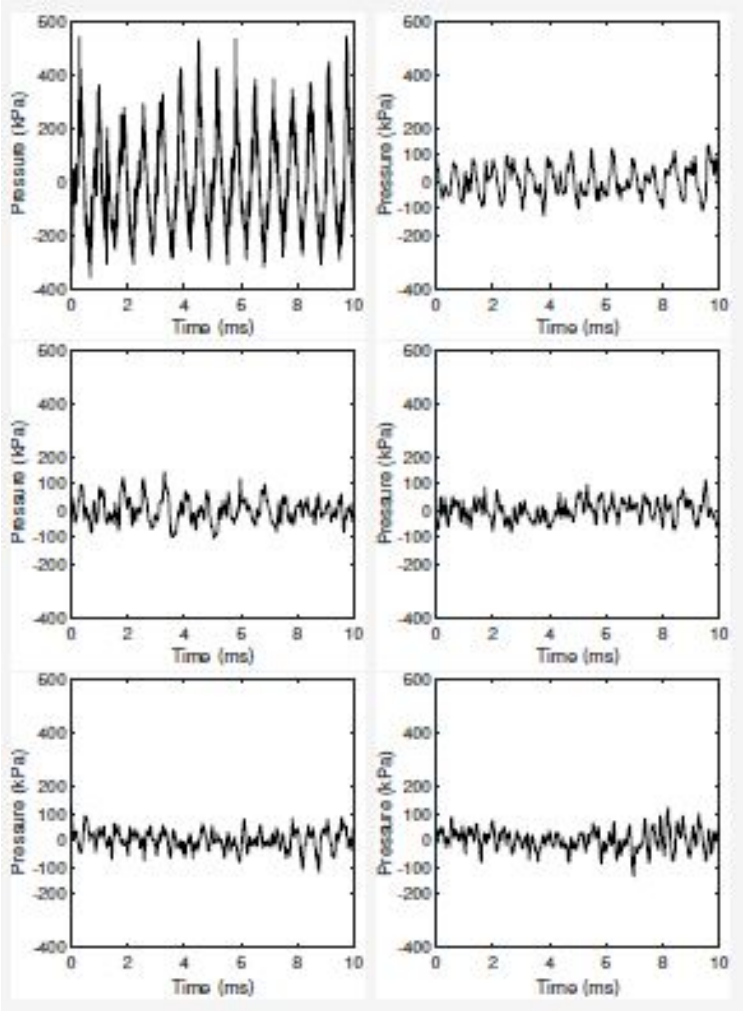

Time-Averaged Fuel Behaviors

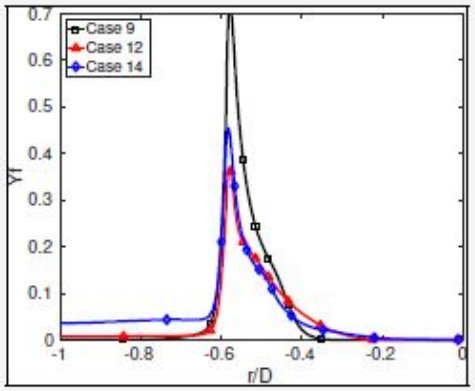

x=0 cm, current solver

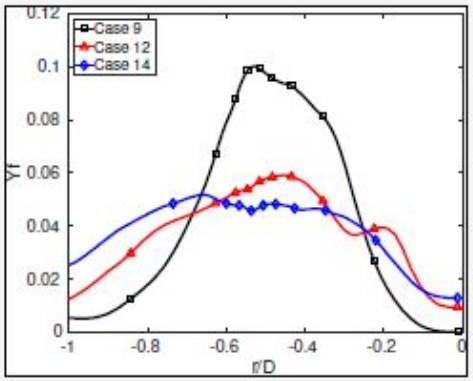

x= 3.08 cm, current solver

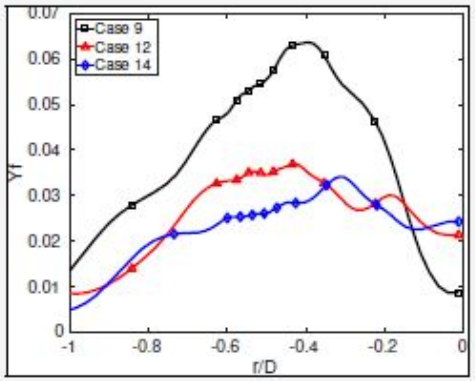

x=6.15 cm, current solver

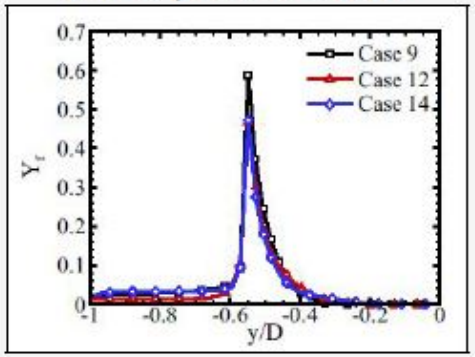

x=0 cm, Srinivasan et at.

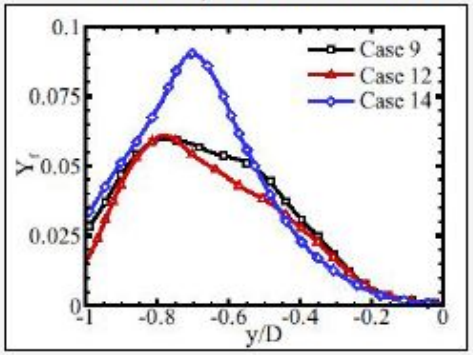

x= 3.08 cm, Srinvasan et al.

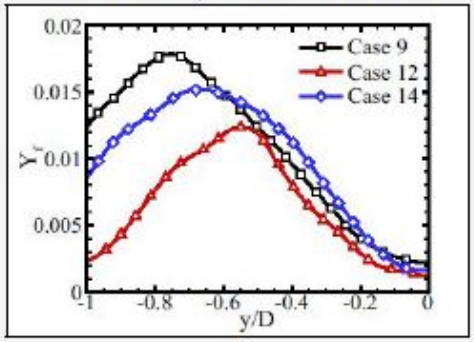

x=6.15 cm, Srinivasan et al.

Instability Mechanisms

- Compare 3 cases
  - 14-cm constant pressure
  - 9-cm choked nozzle (9C)
  - 14-cm choked nozzle (14C)
- Rayleigh index

$$R.I = \frac{1}{\tau}\int_{t}^{t+\tau} \frac{\gamma-1}{\gamma} p' \, \dot{\omega}_T' dt$$

- Vortex shedding
  - $f_v = 800\ Hz \ \rightarrow St = 0.0878$
  - $f_v = 1397\ Hz \ \rightarrow St = 0.1229$
  - $f_v = 1546\ Hz \ \rightarrow St = 0.1316$
- Strouhal number
  - $St = \frac{f_v D}{U}$
  - Preffered mode: 0.1-0.3

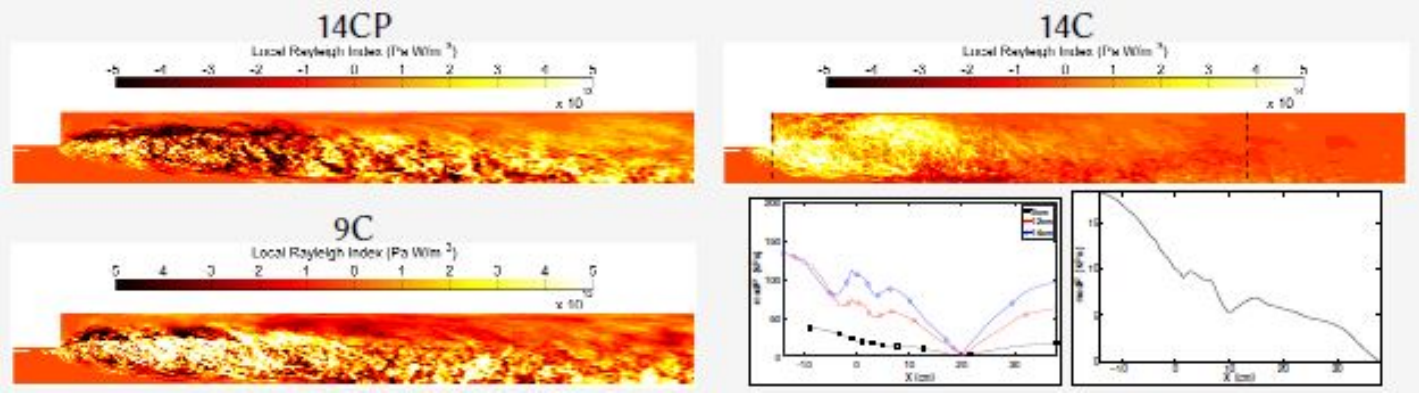

Low Probability Triggered Instabilities

Background – There is a significant probability for triggered instability by

- **a single stochastic disturbance of short duration and large amplitude**
- **two sequential stochastic acceleration disturbances of short duration and smaller amplitude but of synergistic phase.**

New Problem: Triggering by a continuing noise-level disturbance

The probability of instability by a stochastic vibration disturbance of very low amplitude and very long duration (acceleration noise) exists albeit low.

Acceleration profile taken as a smoothed Wiener process over [0, t_d]

$$\mathbf{a}^C(t_i < t < t_{i+1}) = cos^2\left(\frac{\pi(t-t_i)}{2t_s}\right)\mathbf{A}_i + sin^2\left(\frac{\pi(t-t_i)}{2t_s}\right)\mathbf{A}_{i+1}, \;\; \mathbf{A}_i \sim \mathcal{N}(0, \sigma^2 I_2)$$

Approach: **Standard Monte Carlo is ineffective for rare events.**

Introduce a proposal distribution that emphasizes samples more likely to cause instability. Proposal distribution is based on modifying

$$\mathbf{A}_i \sim \mathcal{N}(m_i, \sigma^2 I_2), \;\; \mathbf{m}_i = \frac{2m/s^2}{atm}\frac{\dot{\mathbf{P}}_{i-1}}{\left\|\dot{\mathbf{P}}_{i-1}\right\|} \times max\left(20atm - \|\mathbf{P}_{i-1}\|, 0\right) \times \frac{t_d}{t_d + 1 - t_i}$$

and adjusting the estimated probability by the Likelihood Ratio:

$$\Pi_i \frac{\mathcal{N}(0, \sigma^2 I_2)}{\mathcal{N}(m_i, \sigma^2 I_2)}$$

Rare Event Results

- **Probability of instability increases with RMS level and duration of the noise; we established an empirical law governing these relations**

- **Probability of instability rises sharply within a small RMS range indicating a critical level separating two phases (suggesting a complex systems criticality phenomenon)**

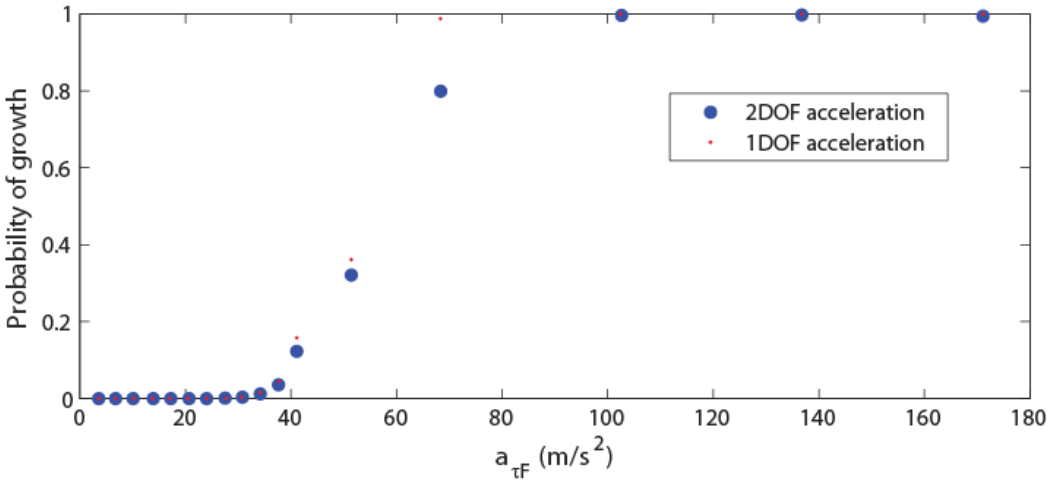

- **For $a_{\tau_F} = 20.6m/s^2,\ t_d = 20ms,\ t_s = 0.01ms$ we computed a 95% Confidence Interval [1.01e-4, 1.22e-4]; this result was achieved with 2000 samples 37% of which were unstable (MC would require 4 million for this calculation)**